Journal of South American Earth Sciences xxx (xxxx) xxx

Contents lists available at ScienceDirect

Journal of South American Earth Sciences

journal homepage: www.elsevier.com/locate/jsames

Provenance of late Paleozoic glacial/post-glacial deposits in the eastern Chaco-Paraná Basin, Uruguay and southernmost Paraná Basin, Brazil

Nicholas D. Fedorchuk[a,b,*], Neil P. Griffis[c], John L. Isbell[b], César Goso[d], Eduardo L.M. Rosa[b], Isabel P. Montañez[c], Qing-Zhu Yin[c], Magdalena H. Huyskens[c], Matthew E. Sanborn[c], Roland Mundil[e], Fernando F. Vesely[f], Roberto Iannuzzi[g]

[a] *Department of Earth Science, Southern Connecticut State University, New Haven, CT, 06515, USA*
[b] *Department of Geosciences, University of Wisconsin-Milwaukee, Milwaukee, WI, 53211, USA*
[c] *Department of Earth and Planetary Sciences, University of California, Davis, CA, 95616, USA*
[d] *Departamento de Geología Sedimentaria y Aplicada (ICG), Facultad de Ciencias, Universidad de la República, Iguá 4225, CP 11400, Montevideo, Uruguay*
[e] *Berkeley Geochronology Center, Berkeley, CA, 94709, USA*
[f] *Departamento de Geologia, Universidade Federal do Paraná, Curitiba, PR, Caixa Postal 19001, CEP 81531-980, Brazil*
[g] *Centro de Investigações do Gondwana, Instituto de Geociências, Universidade Federal do Rio Grande do Sul, Porto Alegre, RS, 91.509-900, Brazil*

ARTICLE INFO

Keywords:
Late Paleozoic ice age
Detrital zircon geochronology
San Gregorio Formation
Itararé Group
Gondwana
Carboniferous

ABSTRACT

The Paraná Basin, Brazil and the Chaco-Paraná Basin, Uruguay both contain sedimentary records that are critical to reconstructing late Paleozoic ice centers in central Gondwana. The orientations of subglacial landforms and glaciotectonic structures suggest that late Paleozoic glacial deposits in the eastern Chaco-Paraná Basin and the southernmost Paraná Basin are genetically related, as they were likely glaciated by the same ice center. However, the location and extent of the ice center responsible for depositing these sediments are unclear. Furthermore, changes in sediment dispersal patterns between glacial, inter-glacial, and post-glacial intervals are not understood for this region of Gondwana. Therefore, this study utilized U–Pb detrital zircon geochronology to assess the provenance of glacial and post-glacial sediments from the eastern Chaco-Paraná Basin (San Gregorio, Cerro Pelado, Tres Islas Formations) and the southernmost Paraná Basin (Itararé Group). Results show dominant age peaks at ~520–555 Ma, ~625 Ma, 750–780 Ma, and 900–1000 Ma in all samples from the eastern Chaco-Paraná Basin. These zircons are interpreted to have been derived from sources in the Cuchilla Dionisio Terrane and Punta del Este Terrane in southeastern Uruguay, and possibly the Namaqua Belt in southern Namibia. Another important source was likely Devonian sedimentary rocks of the Durazno Group in central/eastern Uruguay. Meanwhile, a sample of the glaciogenic Itararé Group from the southernmost Paraná Basin contains a different detrital zircon signature with peaks at ~580 Ma, ~780 Ma, ~2110 Ma, and ~2500 Ma that closely resembles underlying sedimentary and meta-sedimentary rocks of the Precambrian/Cambrian Camaquã Basin. Detrital zircon ages in the glacial and post-glacial sediments indicate that local sources were dominant. In contrast, zircon ages from relatively ice-distal glaciomarine intervals in the Chaco-Paraná Basin reflect more distal sources to the east and southeast, which indicates a larger drainage catchment opened when glaciers retreated and/or the zone of maximum subglacial erosion shifted. Although most zircon ages in the Chaco-Paraná Basin can be attributed to Uruguayan sources, results support the hypothesis that glaciers emanated from southern Namibia and southeast Uruguay into the Chaco-Paraná Basin. From there, ice flowed northwest into the Paraná Basin and then receded back towards Africa as the paleoclimate warmed. The detrital zircon inventory in our study region is distinct from the eastern Paraná Basin, suggesting at least two unique African source regions for glaciers that deposited sediments in the Paraná and Chaco-Paraná Basins.

* Corresponding author. Department of Earth Science, Southern Connecticut State University, New Haven, CT, 06515, USA.
E-mail address: fedorchukn1@southernct.edu (N.D. Fedorchuk).

https://doi.org/10.1016/j.jsames.2020.102989
Received 28 May 2020; Received in revised form 14 October 2020; Accepted 23 October 2020
Available online 2 November 2020
0895-9811/

1. Introduction

The late Paleozoic ice age (LPIA, late Devonian to late Permian) was a time characterized by unique climate conditions relative to most of Earth's history. Glaciers were present in high-to mid-latitude basins across Gondwana, coinciding with the growth of widespread equatorial forests and mires, as well as an atmosphere defined by low pCO_2 and high pO_2 (e.g. Gastaldo et al., 1996; Isbell et al., 2003; 2012; Raymond and Metz, 2004; Montañez and Soreghan, 2006; Fielding et al., 2008; Montañez and Poulsen, 2013; Frank et al., 2015). Interpretations of glaciation during this period have evolved over the past several decades from the original hypothesis of a single, continental-scale ice sheet

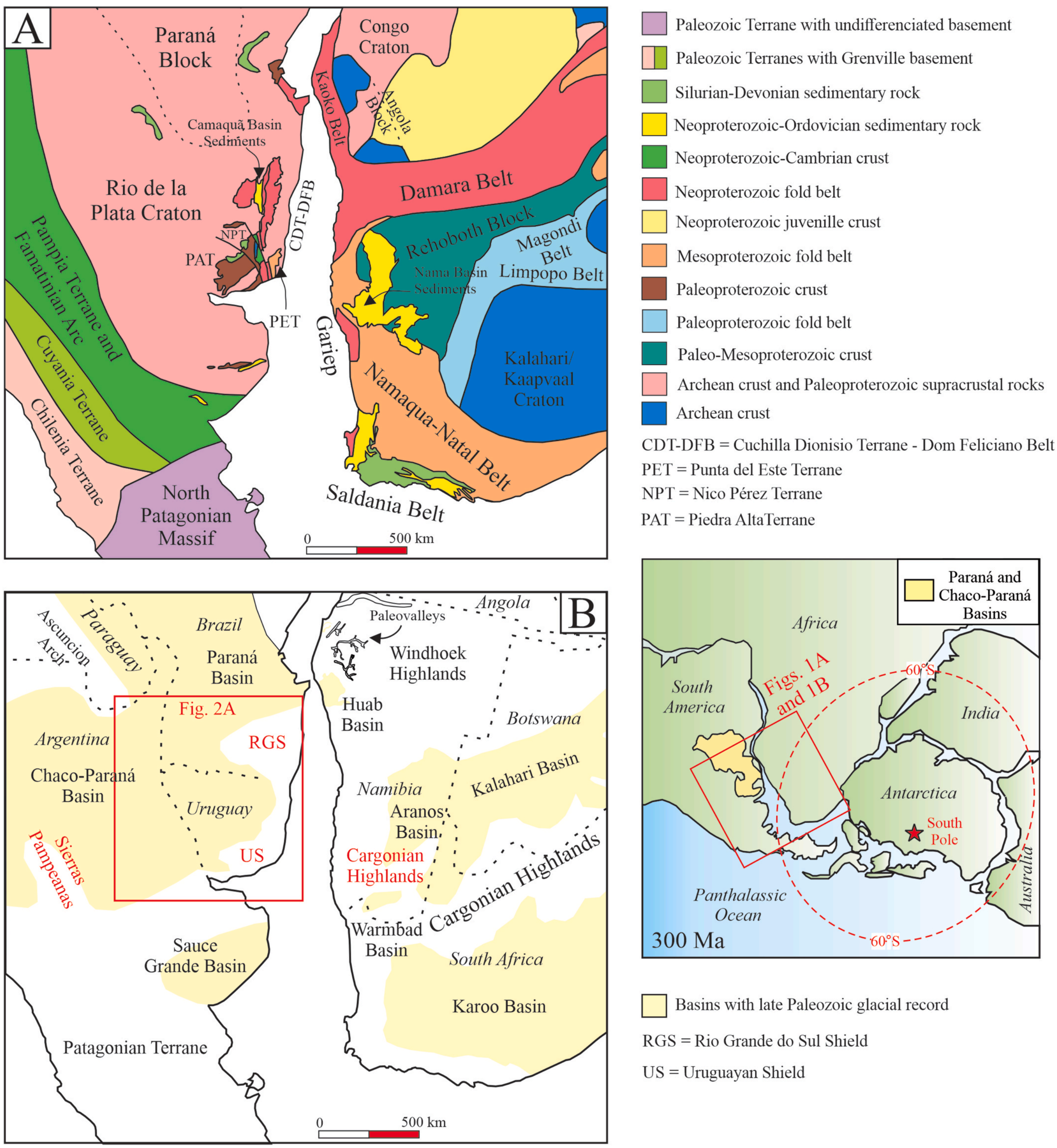

Fig. 1. Paleogeography of Paraná Basin and Chaco-Paraná Basin during late Carboniferous. Plates reconstruction from Lawver et al. (2011). (A) Simplified map of possible source terranes and their ages in South America and southern Africa after Uriz et al. (2016). (B) Map of study area showing late Paleozoic sedimentary basins and paleotopographic highs after Visser (1997b), Winn Jr. and Steinmetz (1998), and Uriz et al. (2016). Possible source areas for sediments examined in this study are in red text (Sierra Pampeanas, RGS, US, Cargonian Highlands). Red box indicates location of Fig. 2a. Dotted black lines represent national borders. (For interpretation of the references to color in this figure legend, the reader is referred to the Web version of this article.)

covering much of Gondwana that persisted for ~100 Myr to a new paradigm of multiple smaller ice sheets and ice caps that fluctuated in time and space on ~1–10 Myr timescales (e.g. Isbell et al., 2003; 2012; Fielding et al., 2008). However, the true nature of the glacial interval, including ice extent, the role of the various climate drivers, and the timing of fluctuations in ice volume, remains unclear.

Considerable work has been done on the LPIA glacial record of individual basins across Gondwana, providing new levels of insight into the sedimentary processes and intrabasinal correlations (e.g. Lopez-Gamundi, 1997; Visser, 1997a; Vesely and Assine, 2006; Fielding et al., 2010; Griffis et al., 2019b). Despite these advances, the temporal and physical connections between strata in adjacent basins remain poorly understood due to the lack of reliable radiometric ages and well constrained biostratigraphic zonations. However, the introduction of detrital zircon geochronology as a tool to assess the provenance of glacial strata allows for improved understanding of paleo-drainage

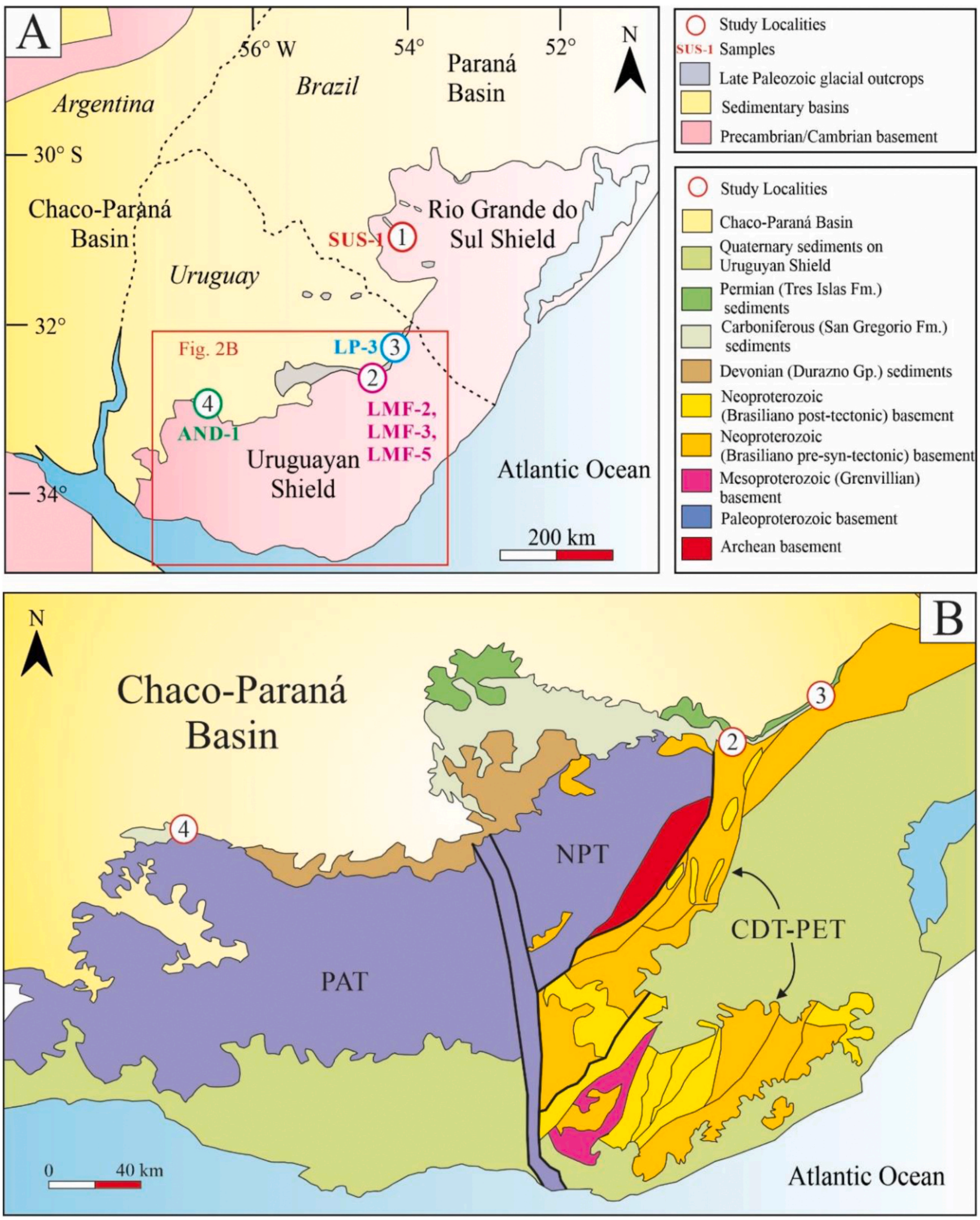

Fig. 2. Study area on Rio Grande do Sul Shield and Uruguayan Shield. (A) Study area with late Paleozoic glacial outcrops in gray after Assine et al. (2018). Study locations indicated by colored circles and samples collected from each location labeled in matching color. Dotted black lines represent national borders. (B) Possible source terranes within Uruguayan Shield after Loureiro et al. (2017) and Blanco et al. (2009). CDT = Cuchilla Dionisio Terrane, PET=Punta del Este Terrane, NPT= Nico Pérez Terrane, PAT = Piedra Alta Terrane. Bold black lines represent major faults. (For interpretation of the references to color in this figure legend, the reader is referred to the Web version of this article.)

patterns, ice extent, and the interbasinal connections between seemingly disparate deposits (e.g. Canile et al., 2016; Craddock et al., 2019; Griffis et al., 2019a; Martin et al., 2019; Tedesco et al., 2019). In particular, one critical area to this line of research is the cross-Atlantic correlation of late Paleozoic glacial sediments in Africa and South America. Two basins long known to be relevant to this question are the Paraná and Chaco-Paraná Basins, which were located on the border between present-day Africa and South America during the late Paleozoic (Fig. 1). The orientation of glacial striations and landforms in these basins were originally used by Du Toit (1927, 1937) as evidence to support the hypothesis of continental drift.

The Paraná Basin is an intracratonic sedimentary basin located in Brazil, Paraguay, Uruguay, and Argentina while the Chaco-Paraná Basin is an intracratonic basin located in Uruguay, Paraguay, and Argentina (e.g. Guillemain, 1911; França and Potter, 1991; Goso, 1995; de Santa Ana, 2004; de Santa Ana et al., 2006a, 2006b; Limarino and Spalletti, 2006; Limarino et al., 2014; Assine et al., 2018). The Chaco-Paraná Basin is connected to the main body of the Paraná Basin near the Brazil-Uruguay-Argentina border (Fig. 1) (Winn Jr. and Steinmetz, 1998). Both basins contain a Carboniferous-Permian glacial record and are thought to have a closely related depositional history (e.g. Assine et al., 2018). However, the glacial record in the Chaco-Paraná Basin is significantly understudied compared to the Paraná Basin due to the scarcity of outcrop exposure (e.g. Winn Jr. and Steinmetz, 1998). The basins are partially separated by a paleotopographic high over the Rio Grande do Sul Shield (or Sul-Riograndense Shield, RGS) that contains isolated outcrops of Carboniferous glacial sediments (Fig. 2) (e.g. Tomazelli and Soliani Júnior 1982; 1997; Fedorchuk et al., 2019a).

Northeast of the RGS, on the eastern margin of the Paraná Basin (Brazil), the predominant east/west and southeast/northwest orientations of subglacial grooves and striations, combined with paleocurrent orientations and ice marginal deformation structures, have long implied that an African-based ice center drained into the eastern Paraná Basin (e.g. Frakes and Crowell, 1972; Crowell and Frakes, 1975; Rocha-Campos et al., 2008, Vesely et al., 2015; Mottin et al., 2018; Rosa et al., 2016, 2019). Furthermore, westward draining paleovalleys with glaciogenic infill have been described in northwest Namibia (Fig. 1B), an area considered to have been connected to the eastern Paraná Basin (e.g. Martin, 1981; Visser, 1997b). In support of this hypothesis, recent detrital zircon geochronology studies have indicated that the glacial sediments on the eastern margin of the Paraná Basin have a Namibian provenance (e.g. Canile et al., 2016; Griffis et al., 2019a). In contrast, detrital zircons from the southernmost margin of the Paraná Basin, collected from the RGS, have a completely different age distribution that indicates a more restricted, local provenance (Fedorchuk et al., 2019b; Griffis et al., 2019a; Tedesco et al., 2019). When this distinction is combined with the most north and northwest flow directions of grooved surfaces and other ice-flow indicators located on the RGS, a separate ice center for the southernmost Paraná Basin (and by extension, the Chaco-Paraná Basin) is suggested in comparison to the eastern margin of the Paraná Basin (e.g. Crowell and Frakes, 1975; Tomazelli and Soliani Júnior 1982, 1997; Crowell, 1999; Fedorchuk et al., 2019a; Tedesco et al., 2019). In particular, the occurrence of proglacial sediments on the RGS with evidence of ice-thrust features support the interpretation of ice advance to the northwest, out of Uruguay (Fedorchuk et al., 2019a). Despite this, the ice center's location and extent responsible for glaciation in the southernmost Paraná and Chaco-Paraná Basins remain unclear.

Although there are scattered outcrops of LPIA glacial deposits in the eastern Chaco-Paraná Basin (Fig. 2), no previous study has analyzed these sediments' provenance. Therefore, detrital zircon samples were collected from these sediments in Uruguay and on the RGS for U–Pb dating by laser ablation inductively-coupled-plasma mass spectrometry (LA-ICP-MS). The goals of this project were to: (1) test the hypothesis that glaciers, separate from the eastern margin of the Paraná Basin, flowed into the Chaco-Paraná Basin and the southern Paraná Basin, (2) constrain ice extent and location by comparing the detrital zircon age distributions to other studies to determine whether glacial sediments in the Chaco-Paraná Basin have a local provenance, an African provenance, or a provenance from elsewhere in South America, and (3) determine if the provenance of the sediments changed during the shift from glacial to post-glacial conditions, reflecting a widespread shift in sediment dispersal patterns.

2. Geologic setting

The Paraná and Chaco-Paraná Basins, which were situated between 45 and 55° south latitude during the Carboniferous, combine to form the largest depocenter of late Paleozoic strata in South America. Paleozoic glacial strata in the Paraná Basin of Brazil are part of the Itararé Group (Fig. 3), which consists of three formations: the Lagoa Azul, Campo Mourão, and Taciba Formations (e.g. França and Potter, 1991). Only the youngest of these, the Taciba Formation, is exposed in the southernmost part of the basin that is featured in this study (e.g. França and Potter, 1991; Holz et al., 2010). The lithologically equivalent LPIA glacial strata in the Chaco-Paraná Basin (Uruguay) is referred to as the San Gregorio and Cerro Pelado Formations (Fig. 3) (e.g. Bossi, 1966; Goso, 1995; de Santa Ana, 2004; de Santa Ana et al., 2006a; 2006b; Assine et al., 2018). Both the Itararé Group and San Gregorio Formation are characterized by glacially-influenced facies associations that include sandstones, rhythmites with dropstones, grooved/striated surfaces interpreted as subglacial erosional features, conglomerates, and diamictites with striated and faceted clasts (e.g. de Santa Ana, 2004; de Santa Ana et al., 2006a; 2006b; Rocha-Campos et al., 2008; Vesely et al., 2015; Assine et al., 2018).

On the RGS, the Itararé Group overlies Precambrian igneous and metamorphic terranes including the Taquarembó Block, the Porongos Belt, the São Gabriel Terrane, and the Pelotas Batholith, as well as Neoproterozoic and Cambrian sedimentary and volcanic rocks of the Camaquã Basin (Fig. 3) (e.g. Gastal et al., 2005; Saalmann et al., 2005, 2006, 2011; Hartmann et al., 2011). In Uruguay, outcrops of the San Gregorio Formation overlie several Precambrian igneous and metamorphic terranes including the Cuchilla Dionisio Terrane, the Nico Pérez Terrane, and the Piedra Alta Terrane (e.g. Santos et al., 2003; Mallmann et al., 2007; Gaucher et al., 2008; Saalmann et al., 2011). The San Gregorio Formation also rests on Devonian sedimentary rocks of the Durazno Group (Fig. 3) (e.g. Uriz et al., 2016).

On the RGS, the postglacial unit that directly overlies the Itararé Group is the coal bearing Rio Bonito Formation (e.g. Holz, 2003; Holz et al., 2006). The Rio Bonito Formation in southernmost Brazil consists of alluvial fan, fluvial-deltaic, and estuarine sediments (e.g. Holz et al., 2006; Fedorchuk et al., 2019b). Radiogenic U–Pb ages of zircons have been measured from ash fall beds and tonsteins within the Rio Bonito Formation. These ages place the Itararé Group/Rio Bonito Formation contact very close to the Gzhelian/Asselian boundary (Fig. 3), thus constraining glaciation on the RGS to the Carboniferous (e.g. Cagliari et al., 2016; Griffis et al., 2018). In Uruguay, the San Gregorio Formation interfingers with and is topped by glaciomarine sediments of the Cerro Pelado Formation and the postglacial, fluvial-deltaic Tres Islas Formation that pinches out to the west. These are considered the lithologic equivalents of the upper Taciba and lower Rio Bonito Formations in the neighboring Paraná Basin (e.g. de Santa Ana, 2004; de Santa Ana et al., 2006a, 2006ba). The lack of ash beds in the San Gregorio, Cerro Pelado, or Tres Islas Formations means that the only age constraints on the glaciation in the Chaco-Paraná Basin are placed by biostratigraphy. Some researchers consider the glacial deposits of the San Gregorio Formation to have been deposited entirely in the Carboniferous on the basis of marine fauna, while others consider deposition to have extended into the early Permian based on the palynology (e.g. Closs, 1967a, 1967b, 1969; Marques-Toigo, 1970, 1974; Beltan, 1981; Braun et al., 2003; Beri et al., 2011, 2015).

Several hypotheses exist for the location and extent of an ice center

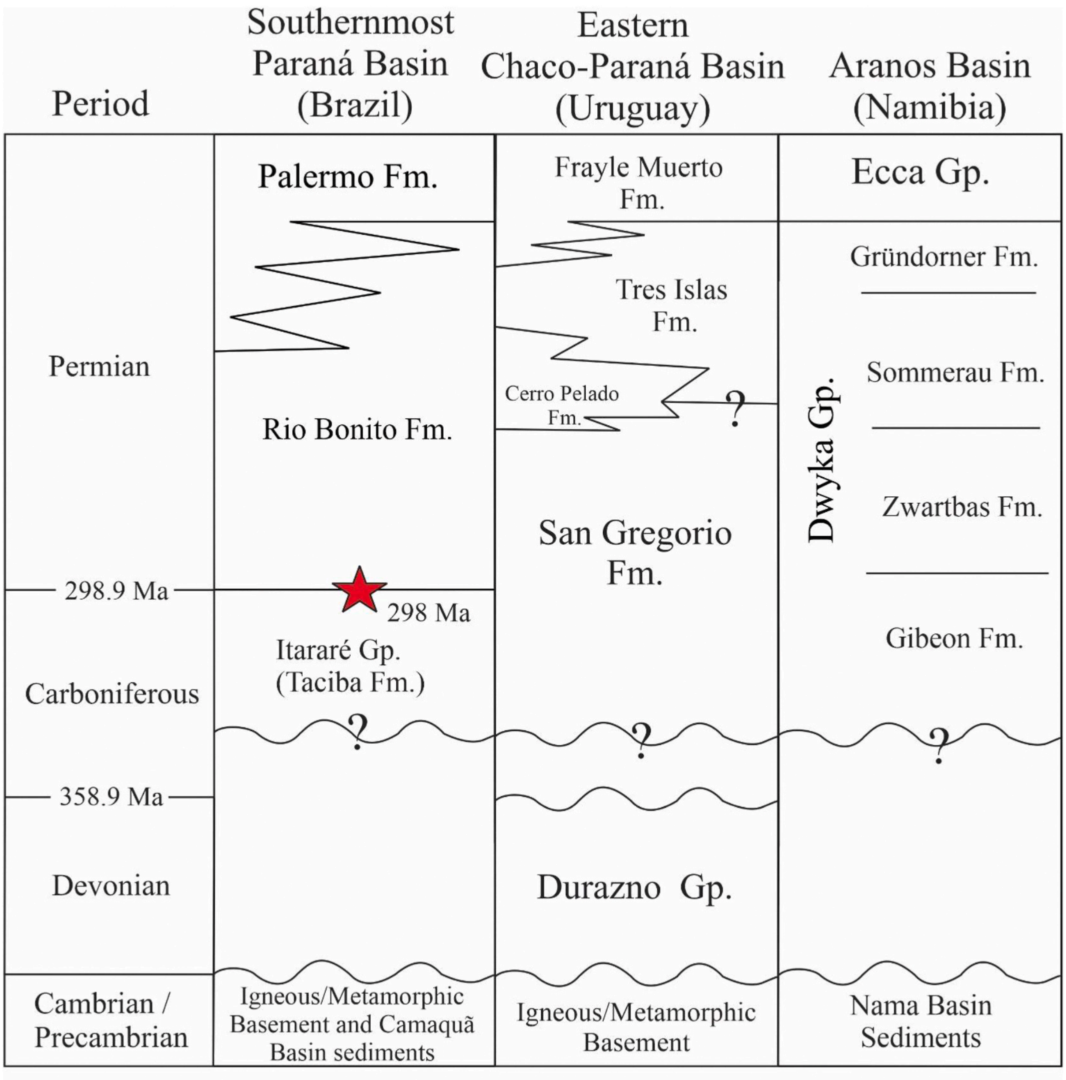

Fig. 3. Stratigraphy of southernmost Paraná Basin, eastern Chaco-Paraná Basin, and Aranos Basin after Holz et al. (2006), de Santa Ana (2004, 2006a) and Zieger et al. (2019, 2020). Red star indicates U–Pb zircon age collected by Griffis et al. (2018). (For interpretation of the references to color in this figure legend, the reader is referred to the Web version of this article.)

that supplied sediment to the RGS and the Chaco-Paraná Basin. One scenario, which is typical of traditional views of the LPIA, suggests that a single massive ice center over Africa or Antarctica spread uniformly westward into the Chaco-Paraná and Paraná Basins (Gesicki et al., 1998, 2002; Starck and Papa, 2006; Holz et al., 2008). Another hypothesis illustrates at least two separate ice centers that spread multiple unconfined lobes onto the eastern and southern margins of the Paraná Basin (e.g. Frakes and Crowell, 1972; Crowell and Frakes, 1975; Assine et al., 2018; Fedorchuk et al., 2019a,b). The later hypothesis commonly portrays a northern ice center over the Windhoek Highlands in northern Namibia, and a southern ice center over the Cargonian Highlands in southern Namibia and South Africa (Fig. 1). A third hypothesis envisions ice that entered the Chaco-Paraná Basin and southernmost Paraná Basin to have been confined to a network of paleofjords draining off Africa (e.g. Tedesco et al., 2016; Fallgatter and Paim, 2017). Finally, a fourth hypothesis depicts multiple small ice caps or sheets on locally uplifted areas around South American basins (e.g. Santos et al., 1996; Rocha-Campos et al., 2008). Potential sediment source areas for the southernmost Paraná Basin and eastern Chaco-Paraná Basin that have been interpreted as paleotopographic highs include the RGS (Brazil), the Pampean Arch (Argentina), and the Cargonian Highlands (southern Namibia) (Fig 1B; e.g. Winn Jr. and Steinmetz, 1998; Visser, 1997b; Rocha-Campos et al., 2008).

3. Location

Samples were collected from a total of four localities that include one location on the RGS (Paraná Basin, Brazil) and three locations in the eastern Chaco-Paraná Basin, Uruguay (Fig. 2). The RGS sample was collected from a glaciotectonized complex of Itararé Group (Taciba Formation) sediments in the Lavras do Sul Municipality, Rio Grande do Sul State (Location 1) (Fig. 2). The sedimentology and stratigraphy of this locality were described in detail by Tomazelli and Solianí Jr (1997) and Fedorchuk et al. (2019a) (Fig. 4). The mean orientation of paleocurrents at Location 1 is to the northwest at 312.2 ± 10.2° (1σ) (Fig. 4). Two of the Uruguayan localities (Locations 2 and 3) are situated in the Cerro Largo Department, outside the city of Melo (~50 km from the Brazil/Uruguay border) (Fig. 2). Location 2 was described in detail by Assine et al. (2018) and contains large subglacially carved "whaleback" structures, oriented between ~320° and 330° carved into igneous basement. Sandstones and diamictites of the San Gregorio Formation overlie these whalebacks and contain multi-directional iceberg keel marks carved into bedding planes (Fig. 4). This location also contains an outcrop of the postglacial Tres Islas Formation that overlies the

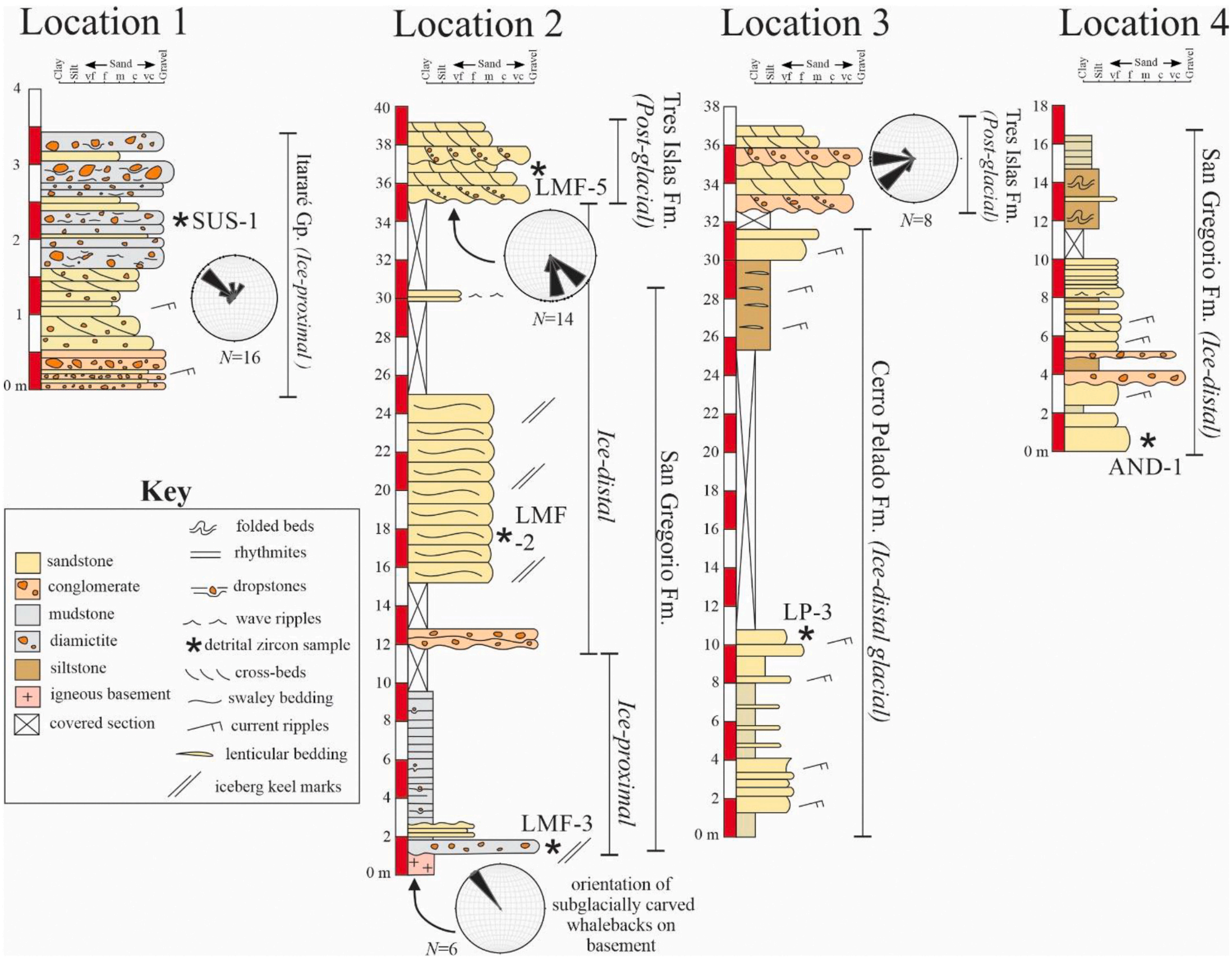

Fig. 4. Stratigraphic columns from study sample locations after Goso (1995), Assine et al. (2018), and Fedorchuk et al. (2019a). Environmental interpretations (ice-proximal glacial, ice-distal glacial, and post-glacial) in italics. Detrital zircon sample locations shown with asterisks and paleocurrent orientations collected from cross-stratification depicted using rose diagrams.

glaciogenic sediments. Paleocurrent data collected from the Tres Islas Formation at Location 2 indicates a flow towards the southeast at 155 ± 12.8° (1σ) (Fig. 4). Meanwhile, Location 3 was described by Goso (1995) and contains outcrops of the Cerro Pelado Formation overlain by coarse fluvial sandstones of the Tres Islas Formation (Figs. 2 and 4). Measurements of paleocurrents in the Tres Islas Formation at Location 3 reveal flow to the southwest at 251 ± 23.6° (1σ) (Fig. 4). Finally, Location 4 is an abandoned quarry outside of the town of Andresito (Uruguay, ~300 km southwest of Locations 2 and 3) that contains the San Gregorio Formation (Figs. 2 and 4).

4. Methods

In total, six samples were collected and analyzed for provenance in this study (SUS-1, LMF-2, LMF-3, LMF-5, LP-3, and AND-1). Sample SUS-1 is from a clast-rich sandy diamictite of the Itararé Group (Taciba Formation) at Location 1 (RGS, Brazil) (Fig. 4) (e.g. Hambrey and Glasser, 2003). LMF-2 and LMF-3 are from the San Gregorio Formation at Location 2 (Uruguay) (Fig. 4). LMF-3 is a sample of clast-rich intermediate diamictite that immediately overlies striated whaleback structures. LMF-2 was collected from a medium, quartz sandstone bed with soft-sediment grooves (interpreted in this study as iceberg keel marks) that is located stratigraphically ~15 m above LMF-3 (Fig. 4). LMF-5 was taken from a cross-bedded, arksosic, medium sandstone of the post-glacial Tres Islas Formation at Location 2 that is located stratigraphically ~10 m above LMF-2 (Fig. 4). LP-3 is from a very fine quartz sandstone bed in the glaciomarine Cerro Pelado Formation at Location 3 (Uruguay) (Fig. 4). Finally, AND-1 is from a fine quartz sandstone bed in the San Gregorio Formation at Location 4 (Uruguay) (Fig. 4).

The provenance of these samples was determined by U–Pb detrital zircon geochronology. The samples were all analyzed by laser ablation inductively coupled plasma mass spectrometry (LA-ICP-MS) at the University of California, Davis. A complete description of the zircon separation and ablation methods and complete data is found in the supplemental files. Samples were compared to each other and to possible sources using the Kolmogorov-Smirnov (K–S) Test with error in the Cumulative Distribution Function (CDF), sample CDFs, cross-correlation coefficients from probability density plots (PDPs) of the samples, and multidimensional scaling (MDS) (e.g. Saylor and Sundell, 2016; Vermeesch et al., 2016). For the K–S Test, a P-value of <0.05 indicates with 95% confidence that the two age distributions are not the same. However, this test cannot assess if the samples have the same provenance (e.g. Berry et al., 2001; DeGraaff-Surpless et al., 2003; Saylor and Sundell, 2016). The cross-correlation coefficient is the coefficient of determination of a cross-plot of two PDPs for the same age range (e.g. Saylor et al., 2012, 2013; Saylor and Sundell, 2016). For this test, an R^2 value will range from 0 to 1 whereby a value close to 1 means that the PDPs are very similar, with closely matching age peaks and peak heights. Kernel Density Plots (KDEs) with adaptive bandwidths were used for visual comparison of samples since their peaks are smoother than PDPs and less likely to contain small peaks that make it difficult to identify broad patterns (Figs. 5–7) (e.g. Saylor and Sundell, 2016; Vermeesch et al., 2016). Multidimensional scaling (MDS) is similar to a principle component analysis. This test reproduces relative ranks of dissimilarity between samples so that samples more similar to each other plot closer together and samples more dissimilar to each other plot farther apart (e.g. Vermeesch et al., 2016). MDS, KDE, and CDF plots were created using *provenance*, a free package for *R* (Vermeesch et al., 2016). Cross-correlation coefficients were calculated using the *DZ Stats* compiler for *Matlab* (e.g. Saylor and Sundell, 2016). Although all of these statistical comparisons are useful, it should be noted that in relatively small-*N* samples (<300) and samples with variable *N*, such as those in this study, the cross-correlation coefficient is considered the most sensitive metric of similarity (e.g. Saylor and Sundell, 2016).

To place detrital zircon samples in their proper stratigraphic context, most samples were collected from measured sections describe in previous studies (i.e. Locations 1, 2, and 3) (Goso, 1995; Assine et al., 2018; Fedorchuk et al., 2019a). Location 4 is from a previously undescribed section so a new stratigraphic column was measured. The stratigraphic position of each sample is shown next to the stratigraphic column of the locality from which it was collected (Fig. 4).

5. Results

5.1. Detrital zircon U–Pb ages

5.1.1. Sample SUS-1 (Location 1, Itararé Group, Paraná Basin)

The KDE ($N = 53$) of sample SUS-1 shows a dominant Neoproterozoic peak at ~580 Ma with much smaller (and broader) secondary peaks at ~780 Ma, ~2110 Ma, and ~2500 Ma (Fig. 5). In this sample, 2% of the zircons analyzed were Ordovician, 74% were Neoproterozoic, 2% were Mesoproterozoic, and 22% were Paleoproterozoic (Fig. 8).

5.1.2. Sample LMF-3 (Location 2, San Gregorio Formation, Chaco-Paraná Basin)

The KDE of LMF-3 ($N = 59$) exhibits a dominant peak at ~625 Ma and a secondary peak at ~520 Ma. Less constrained peaks occur at ~750 Ma, ~990 Ma, and ~1850 Ma (Fig. 6). LMF-3 contains 24% Cambrian grains, 63% Neoproterozoic grains, 7% Mesoproterozoic grains, 5% Paleoproterozoic grains, and 1% Archean grains (Fig. 8).

5.1.3. Sample LMF-2 (Location 2, San Gregorio Formation, Chaco-Paraná Basin)

The KDE of sample LMF-2 ($N = 73$) has a primary peak at ~555 Ma and a secondary peak at ~650 Ma. Smaller and broader peaks occur at ~780 Ma, ~1250 Ma, and ~1890 Ma (Fig. 6). LMF-2 contains 16% Cambrian grains, 72% Neoproterozoic grains, 4% Mesoproterozoic grains, and 8% Paleoproterozoic grains (Fig. 8).

5.1.4. Sample LMF-5 (Location 2, Tres Islas Formation, Chaco-Paraná Basin)

The KDE of sample LMF-5 ($N = 50$) shows a primary peak at ~625 Ma and a secondary peak at ~555 Ma (Fig. 6). LMF-5 has a less diverse zircon population when compared to most other samples, with 4% Cambrian grains and 96% Neoproterozoic grains (Fig. 8).

5.1.5. Sample LP-3 (Location 3, Cerro Pelado Formation, Chaco-Paraná Basin)

The KDE of sample LP-3 ($N = 100$) shows a primary peak at ~525 Ma and a secondary peak at ~625 Ma. Smaller and broader third-order peaks are located at ~755 Ma, and ~1010 Ma (Fig. 6). Sample LP-3 contains 26% Cambrian grains, 54% Neoproterozoic grains, 14%

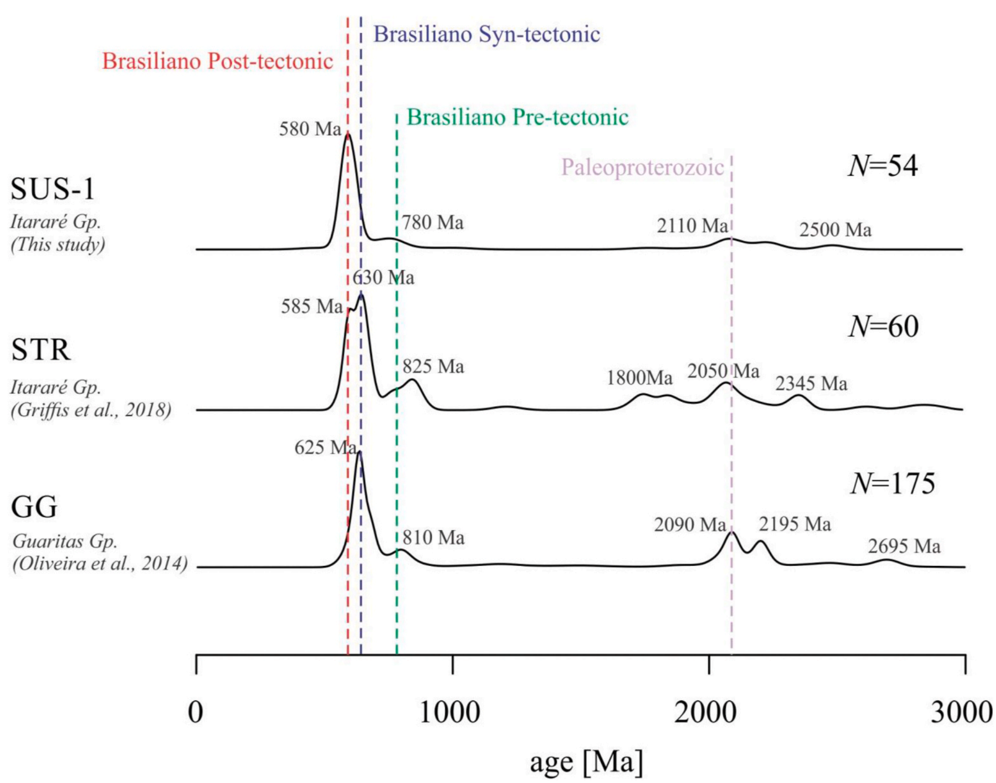

Fig. 5. Kernel density plot of sample SUS-1 compared to other samples from Rio Grande do Sul Shield including sample STR (Griffis et al., 2019a) and sample GG (Oliveira et al., 2014). Similar peaks and relative peaks heights indicates a close provenance relationship between samples. Note the overlapping peaks and similar peak intensities between Itararé Group samples SUS-1 and STR compared to the underlying Camaquã Basin (Guaritas Group) sediments.

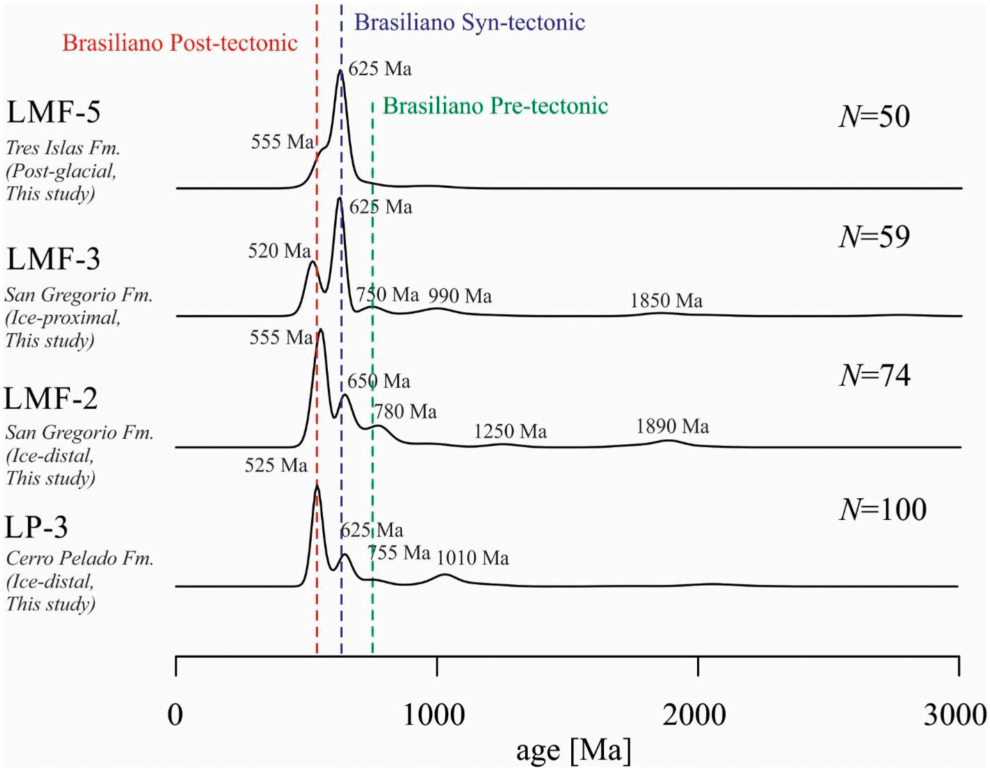

Fig. 6. Kernel density plots of samples LMF-5, LMF-3, LMF-2, and LP-3. Relative changes in the amount of syn-tectonic and post-tectonic zircons between ice-proximal, relatively ice-distal, and post-glacial environments reflects changes to drainage patterns. Similar peaks and relative peaks heights indicates a close provenance relationship between samples.

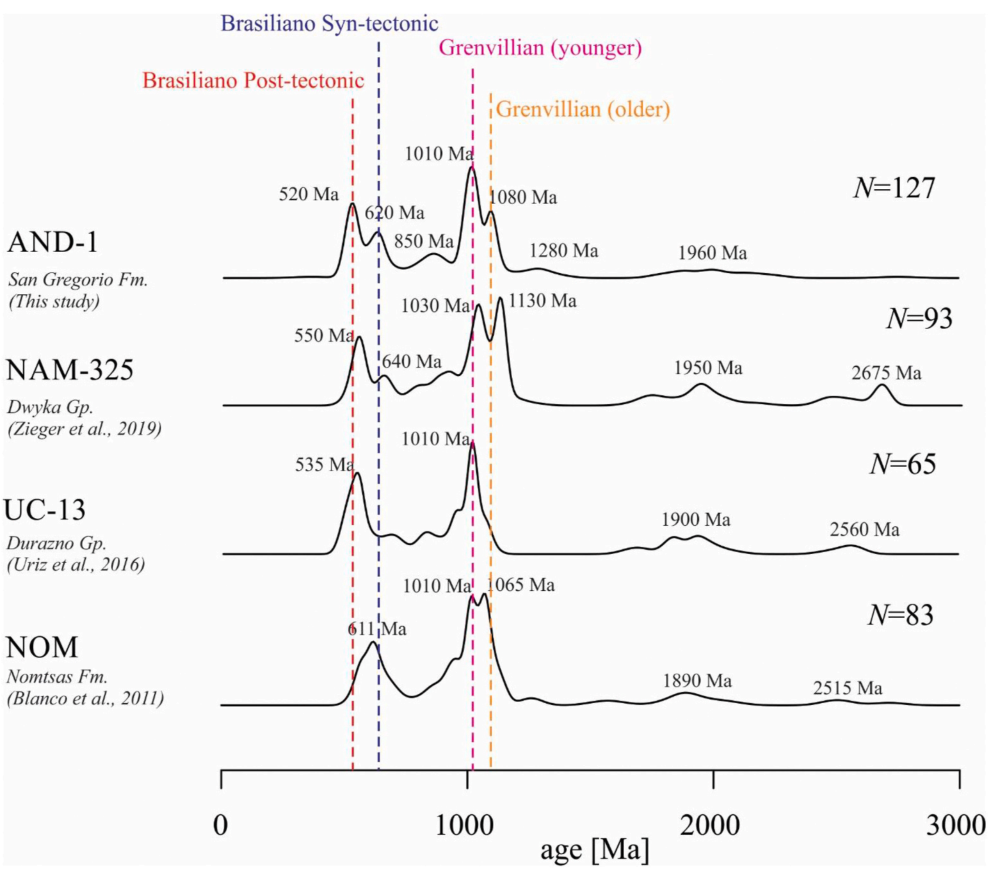

Fig. 7. Kernel density plots of samples AND-1, UC-13 (Uriz et al., 2016), NOM (Blanco et al., 2011), and NAM-325 (Zieger et al., 2019). Sample AND-1 has similar peaks to NAM-325 from the Permian Dwkya Group, UC-13 from Devonian Durazno Group, and sample NOM from Cambrian Nomtsas Formation. Similar peaks and relative peaks heights indicates a shared provenance relationship between samples. Note that sample AND-1 has different detrital zircon ages, including significant Mesoproterozoic peaks, compared with other San Gregorio Formation samples from Locations 2 and 3.

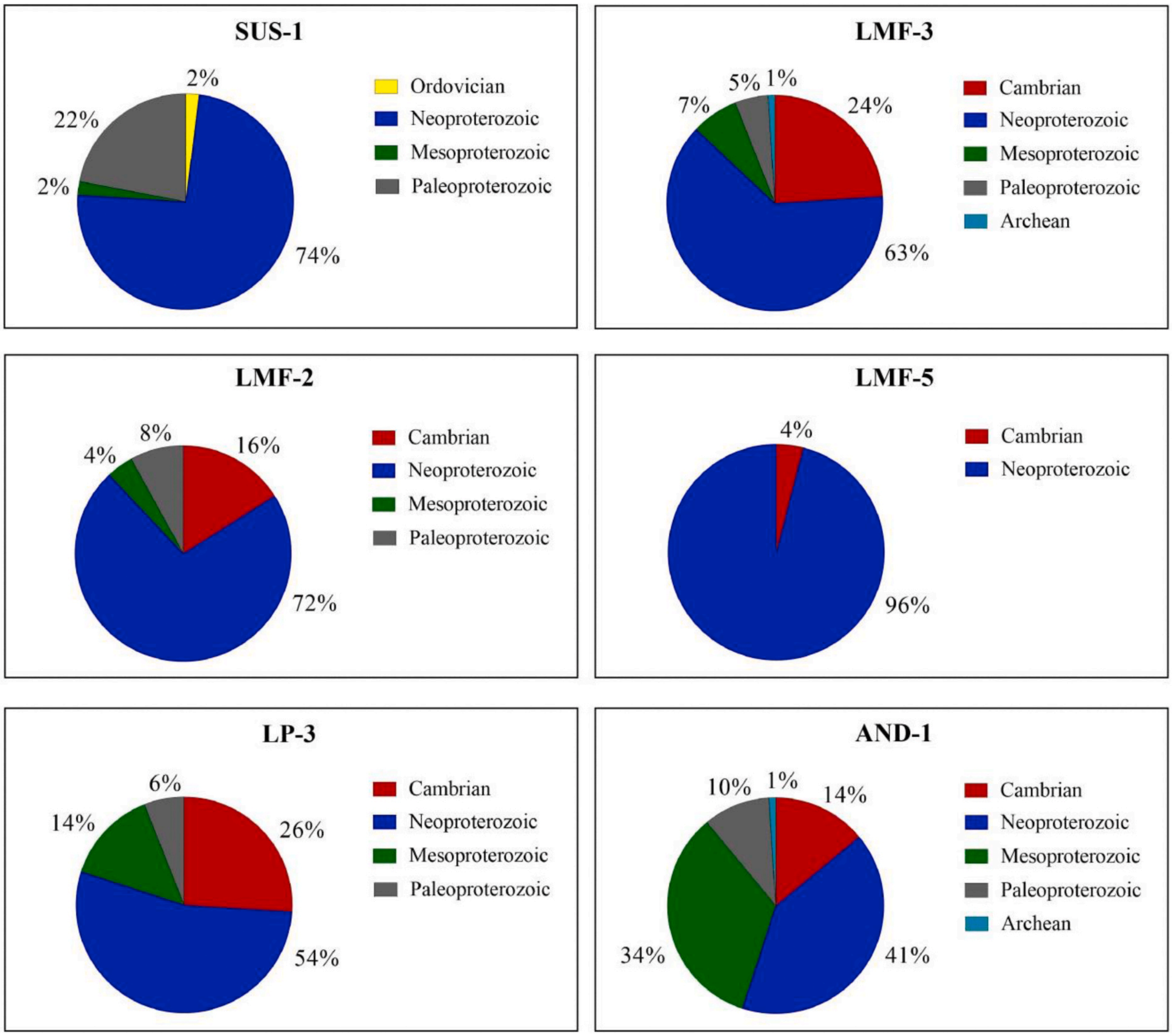

Fig. 8. Pie charts showing percentage of Ordovician, Cambrian, Neoproterozoic, Mesoproterozoic, Paleoproterozoic, and Archean grains in each detrital zircon sample. Note sample LMF-5 has a lack of diverse grains and sample AND-1 is unique for its abundance of Mesoproterozoic grains.

Mesoproterozoic grains, and 6% Paleoproterozoic grains (Fig. 8).

5.1.6. Sample AND-1 (Location 4, San Gregorio Formation, Chaco-Paraná Basin)

The KDE of sample AND-1 ($N = 127$) exhibits a strong primary peak at ~1010 Ma with secondary peaks at ~525 Ma and ~620 Ma. Smaller, less constrained peaks are located at ~850 Ma, 1080 Ma, ~1280 Ma, and ~1960 Ma (Fig. 7). AND-1 contains 14% Cambrian grains, 41% Neoproterozoic grains, 34% Mesoproterozoic grains, 10% Paleoproterozoic grains, and 1% Archean grains (Fig. 8).

5.2. Statistical comparison of samples

Samples were compared to each other using the K–S test (Table 1), the cross-correlation coefficient (Table 2), their CDFs (Fig. 9), and MDS (Fig. 10) to assess potential source regions and variations in drainage. To examine possible source regions for the samples, their age distributions were compared to detrital zircon samples from several prior studies that vary geographically and temporally (Tables 1 and 2, Figs. 9 and 10). These comparative detrital zircon studies include: Carboniferous (Itararé Group) rocks from the Paraná Basin in Brazil (Sample STR, Griffis et al., 2019a), Cambrian sedimentary rocks (Nomtsas Formation, Nama Group) from the Nama Basin in southern Namibia (Sample NOM, Blanco et al., 2011), Neoproterozoic metasedimentary rocks (Guaritas Group) from the Camaquã Basin on the RGS, Brazil (Sample GG, Oliveira et al., 2014), Devonian sedimentary rocks (Durazno Group) from the Chaco-Paraná Basin in Uruguay (Sample UC-13, Uriz et al., 2016), and a Permian diamictite sample (NAM-325) from the glaciogenic Dwyka Group (Gibeon Formation) in the Aranos Basin, Namibia (Fig. 3) (Zieger et al., 2019).

5.2.1. Sample SUS-1

The K–S test indicates that the detrital zircon age distribution of sample SUS-1 cannot be distinguished from samples LMF-3 (San Gregorio Formation), LMF-2 (San Gregorio Formation), and LMF-5 (Tres Islas Formation) (i.e. P-value > 0.05) (Table 1). Similarly, MDS indicates SUS-1 is most closely related to LMF-2 and LMF-3 (Fig. 10). A comparison to all other samples exhibits a P-value of <0.05 and, therefore, it can be said with 95% confidence that the other samples have a different zircon population than SUS-1. In direct contrast to these K–S test and MDS results, sample STR (Itararé Group) from Griffis et al. (2019a) has the highest cross-correlation coefficient ($R^2 = 0.63$) compared to SUS-1 (Table 2). Although this result contradicts the K–S test and MDS, the relatively high R^2 value would seem logical since SUS-1 and STR are both samples of the Itararé Group collected on the RGS. The reason for the contradictory result may be that the small sample sizes of both SUS-1

Table 1
Comparison of K–S P-values between samples analyzed in this study (green) and other studies (red). P-values < 0.05 indicate that two samples were drawn from different populations (i.e. have different provenance). P-values > 0.05 (highlighted in yellow) indicate samples cannot be clearly distinguished as having separate provenance. Sample STR from Carboniferous Itararé Gp on RGS (Griffis et al., 2019a), sample GG from Neoproterozoic Guaritas Group on RGS (Oliveira et al., 2014), sample NOM from Cambrian Nomtsas Formation in Namibia (Blanco et al., 2011), sample UC-13 from Devonian Durazno Group in Uruguay (Uriz et al., 2016), and sample NAM-325 from Permian Dwyka Group in Namibia (Zieger et al., 2019).

	SUS-1	LMF-3	LMF-2	LMF-5	LP-3	AND-1	STR	GG	NOM	UC-13	NAM-325
SUS-1		0.14	0.15	0.06	0.00	0.00	0.00	0.00	0.00	0.00	0.00
LMF-3	0.14		0.21	0.30	0.09	0.00	0.00	0.00	0.00	0.00	0.00
LMF-2	0.15	0.21		0.06	0.61	0.00	0.00	0.00	0.00	0.00	0.00
LMF-5	0.06	0.30	0.06		0.04	0.00	0.00	0.00	0.00	0.00	0.00
LP-3	0.00	0.09	0.61	0.04		0.00	0.00	0.00	0.00	0.00	0.00
AND-1	0.00	0.00	0.00	0.00	0.00		0.00	0.00	0.30	0.73	0.05
STR	0.00	0.00	0.00	0.00	0.00	0.00		0.80	0.01	0.17	0.01
GG	0.00	0.00	0.00	0.00	0.00	0.00	0.80		0.00	0.00	0.00
NOM	0.00	0.00	0.00	0.00	0.00	0.30	0.01	0.00		0.21	0.57
UC-13	0.00	0.00	0.00	0.00	0.00	0.73	0.17	0.00	0.21		0.05
NAM-325	0.00	0.00	0.00	0.00	0.00	0.05	0.01	0.00	0.57	0.05	

Table 2
Comparison of cross-correlation coefficients (R^2) between samples analyzed in this study and other studies. Sample STR from Carboniferous Itararé Gp on RGS (Griffis et al., 2019a), sample GG from Neoproterozoic Guaritas Group on RGS (Oliveira et al., 2014), sample NOM from Cambrian Nomtsas Formation in Namibia (Blanco et al., 2011), sample UC-13 from Devonian Durazno Group in Uruguay (Uriz et al., 2016), and sample NAM-325 from Permian Dwyka Group in Namibia (Zieger et al., 2019).

	SUS-1	LMF-3	LMF-2	LMF-5	LP-3	AND-1	STR	GG	NOM	UC-13	NAM-325
SUS-1		0.29	0.32	0.43	0.13	0.07	0.63	0.47	0.12	0.08	0.05
LMF-3	0.29		0.18	0.58	0.19	0.22	0.36	0.37	0.11	0.09	0.04
LMF-2	0.32	0.18		0.38	0.76	0.17	0.32	0.23	0.10	0.27	0.19
LMF-5	0.43	0.58	0.38		0.25	0.10	0.55	0.56	0.14	0.08	0.06
LP-3	0.13	0.19	0.76	0.25		0.26	0.15	0.12	0.09	0.32	0.24
AND-1	0.07	0.22	0.17	0.10	0.26		0.08	0.08	0.57	0.60	0.49
STR	0.63	0.36	0.32	0.55	0.15	0.08		0.87	0.13	0.06	0.05
GG	0.47	0.37	0.23	0.56	0.12	0.08	0.87		0.12	0.03	0.03
NOM	0.12	0.11	0.10	0.14	0.09	0.57	0.13	0.12		0.46	0.59
UC-13	0.08	0.09	0.27	0.08	0.32	0.60	0.06	0.03	0.46		0.44
NAM-325	0.05	0.04	0.19	0.06	0.24	0.49	0.05	0.03	0.59	0.44	

and STR make the K–S test overly sensitive to their differences. No samples had both cross-correlation coefficients >0.5 and K–S test P-values > 0.05 when compared to SUS-1 (Table 2).

5.2.2. *Sample LMF-3*

The detrital zircon population of sample LMF-3 cannot be distinguished from samples SUS-1 (Itararé Group), LMF-2 (San Gregorio Formation), LMF-5 (Tres Islas Formation) and LP-3 (Cerro Pelado Formation) using the K–S test (Table 1). All the other samples have P-values < 0.05 and therefore are likely to have different provenance. Only sample LMF-5 has a cross-correlation coefficient >0.5 ($R^2 = 0.58$) when compared with sample LMF-3 (Table 2). Based on the agreement of the K–S test and the cross-correlation coefficient, it is hypothesized that the zircon provenance of sample LMF-5 is most similar to sample LMF-3. This is supported by the MDS, which also indicates that LMF-5 is most similar to LMF-3 (Fig. 10).

5.2.3. *Sample LMF-2*

The detrital zircon population of LMF-2 cannot be distinguished from those of samples SUS-1 (Itararé Group), LMF-3 (San Gregorio Formation), LMF-5 (Tres Islas Formation), and LP-3 (Cerro Pelado Formation) using the K–S test (P-values > 0.05) (Table 1). Sample LP-3 has an R^2 value of 0.76 versus LMF-2. Based on the agreement of the K–S test and the cross-correlation coefficient for sample LP-3, it is hypothesized that the provenance of sample LMF-2 is most similar to sample LP-3. Similarly, the MDS shows that LP-3 is closely related to LMF-2 (Fig. 10).

5.2.4. *Sample LMF-5*

The detrital zircon population of LMF-5 cannot be distinguished from samples SUS-1 (Itararé Group), LMF-3 (San Gregorio Formation), and LMF-2 (San Gregorio Formation) based on the K–S test (Table 1). However, samples LMF-3, STR (Itararé Group), and GG (Gauritas Group) all have cross-correlation coefficient's > 0.5 that stand out from the rest of the samples (Table 2). Sample LMF-3 has a R^2 value of 0.58, STR has a R^2 value of 0.55, and GG has a R^2 of 0.56 compared to sample LMF-5. However, only LMF-3 has both a K–S test P-value > 0.05 and a $R^2 > 0.5$, which suggests that LMF-3 has a provenance most similar to LMF-5 (Table 2). Supporting this, the MDS connects LMF-5 to LMF-3 as its nearest neighbor (Fig. 10).

5.2.5. *Sample LP-3*

The detrital zircon population of LP-3 cannot be distinguished from samples LMF-3 (San Gregorio Formation) and LMF-2 (San Gregorio Formation) based on the K–S test (Table 1). LMF-2 has a R^2 value of 0.76 when compared to LP-3. Since LMF-2 has a K–S P-value > 0.05 and R^2 value in agreement, this sample is interpreted to have the most similar

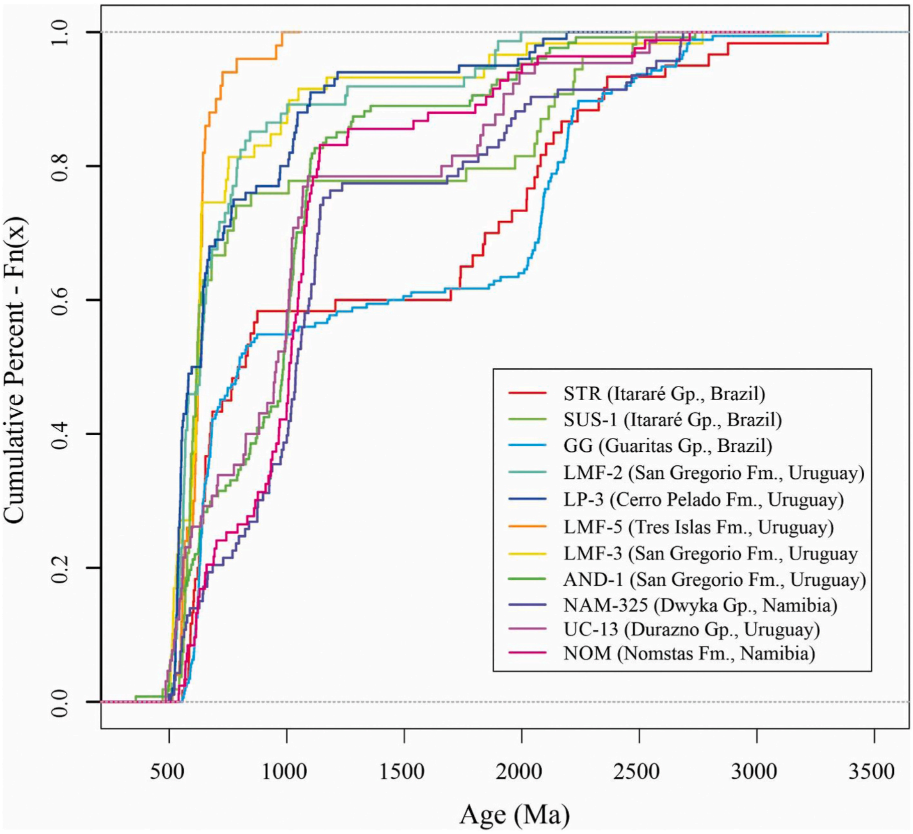

Fig. 9. Cumulative distribution functions of samples analyzed in this study and other studies. Greater space between sample functions indicates increased dissimilarity. Sample STR from Carboniferous Itararé Group on RGS (Griffis et al., 2019a), sample GG from Neoproterozoic Guaritas Group on RGS (Oliveira et al., 2014), sample NOM from Neoproterozoic Cambrian Nomtsas Formation in Namibia (Blanco et al., 2011), sample UC-13 from Devonian Durazno Group in Uruguay (Uriz et al., 2016), and sample NAM-325 from Permian Dwyka Group in Namibia (Zieger et al., 2019).

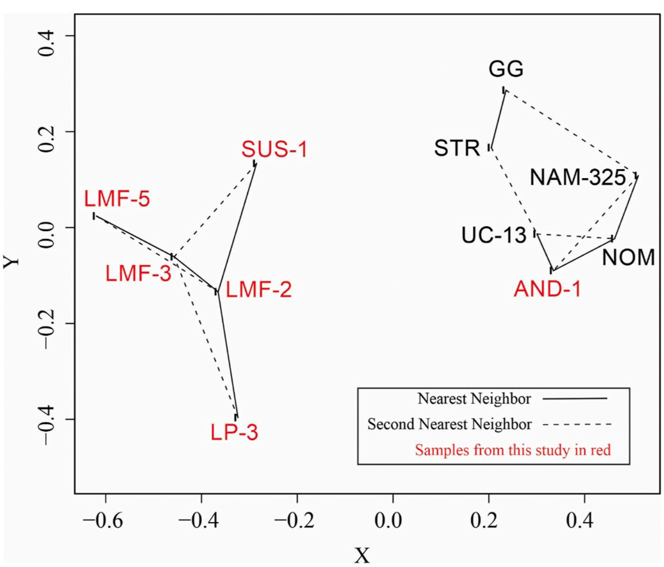

Fig. 10. Multidimensional scaling analysis of samples analyzed in this study (red) and other studies. Samples more similar to each other plot closer together and samples more dissimilar to each other plot farther apart. Sample STR from Carboniferous Itararé Gp on RGS (Griffis et al., 2019a), sample GG from Neoproterozoic Guaritas Group on RGS (Oliveira et al., 2014), sample NOM from Cambrian Nomtsas Formation in Namibia (Blanco et al., 2011), sample UC-13 from Devonian Durazno Group in Uruguay (Uriz et al., 2016), and sample NAM-325 from Permian Dwyka Group in Namibia (Zieger et al., 2019). (For interpretation of the references to color in this figure legend, the reader is referred to the Web version of this article.)

provenance to sample LP-3 (Table 2). The MDS connects LP-3 to LMF-2 as its nearest neighbor (Fig. 10).

5.2.6. *Sample AND-1*

The detrital zircon population of AND-1 cannot be distinguished from samples NOM (Nomtsas Formation), NAM-325 (Dwyka Group), and UC-13 (Durazno Group) using the K–S test (Table 1). NOM and UC-13 have cross-correlation coefficients >0.5 when compared to AND-1. NOM has an R^2 value of 0.57 and UC-13 has an R^2 value of 0.60 (Table 2). It should be noted that NAM-325 (Dwyka Group) has an R^2 value of 0.49 compared to AND-1 and also has the most similar peaks and intensities when comparing their KDE's (Fig. 7). Therefore, samples NOM, UC-13, and NAM-325 are all considered to have similar provenance to AND-1 (Table 2). This interpretation is further supported by the MDS which exhibits nearest neighbor lines connecting AND-1 to both UC-13 and NOM, as well as a second nearest neighbor line connecting AND-1 to NAM-325 (Fig. 10).

6. Discussion

Based on the U–Pb detrital zircon results presented here and interpretations of paleo ice-flow indicators, the most likely source region for the glacial sediments (San Gregorio Formation) deposited in the eastern Chaco-Paraná Basin is the Cuchilla Dionisio Terrane (Uruguay), the Punta del Este Terrane (Uruguay) and, by extension, the Namaqua Belt in Africa, which would have been directly connected to the Punta del Este Terrane during the late Paleozoic (Figs. 1 and 2) (Basei et al., 2011). These terranes were located to the southeast and east of the basin and were likely connected to the Cargonian Highlands that stretched across southern Africa (Fig. 1) (e.g. Visser, 1997b). A comparison of the detrital zircon signature from glacial (ice-proximal), glaciomarine (relatively ice-distal), and postglacial samples exhibits an interesting trend whereby ice-proximal glacial sediments reflect local erosion of underlying sediments or crystalline basement. Meanwhile, more diverse detrital zircon ages from distal sources are found under glaciomarine conditions. Post-glacial fluvial sediments reflect incision of local underlying units and a return to highly local provenance that is similar to that of ice-proximal sediments.

6.1. Comparison of samples to likely source regions

The Cuchilla Dionisio and Punta del Este Terranes are considered here as the most likely source of sediment to the eastern Chaco-Paraná Basin during the LPIA. In the samples from the Chaco-Paraná Basin that were analyzed (i.e. samples LMF-3, LMF-2, LMF-5, LP-3, AND-1) the two most common age peaks were ~520–555 Ma and ~625 Ma. The ~625 Ma ages are typical of syn-tectonic granites of the Cuchilla Dionisio Terrane (Uruguay) which directly underlie the study Locations 2 and 3 and are the most plausible source of zircons (e.g. Blanco, 2009; Basei et al., 2011). Meanwhile, the ~520–555 Ma ages are consistent with nearby post-tectonic granite intrusions (Fig. 2B) to the south and east in the Punta del Este Terrane (Uruguay), such as the El Pintor Granite, José Ignacio Granite, the Rocha Granite, and the Santa Teresa Granite (e.g. Blanco et al., 2009; Basei et al., 2011). Grenvillian ages of ~900–1000 Ma are also found within gneisses of the Cerro Olivo Complex, part of the Punta del Este Terrane and, correlatively, the Namaqua Belt in Africa (e. g. Blanco et al., 2009; Basei et al., 2011). Finally, pre-tectonic Brasiliano ages of ~750–780 Ma are found in migmatites of the Punta del Este Terrane (e.g. Bossi and Gaucher, 2004; Blanco et al., 2009).

The Cuchilla Dionisio Terrane and Punta del Este Terrane are interpreted as extensions of the Gariep Belt and Namaqua Belt in southern Africa that were formed by the collision of the Río de la Plata and Kalahari Cratons during the final assembly of southwest Gondwana in the Neoproterozoic (Fig. 1) (the Brasiliano Orogeny, e.g. Gaucher et al., 2008). These terranes have been previously depicted as highlands that supplied the sediments of the Devonian Durazno Group in eastern Uruguay (e.g Uriz et al., 2016) and were likely connected to the Cargonian Highlands of southern Africa, a paleotopographic high (Fig. 1) (e. g. Visser, 1997b). The Cargonian Highlands have been previously interpreted as a source region for Carboniferous and Permian glaciogenic sediments (Dwyka Group) in southern Namibia (e.g. Zieger et al., 2019). In all the samples analyzed from the eastern Chaco-Paraná Basin, the relatively low abundance (<12%) of Paleoproterozoic grains, which are typical to the Nico Pérez and the Piedra Alta Terranes (Fig. 2B), indicates that rocks to the southwest and west of the Uruguayan Shield were not a significant source of sediment. This tends to rule out the far western Sierra Pampeanas as a significant source region, an interpretation supported by paleo ice-flow indicators and the lack of Silurian and Devonian ages that are common to the Sierra Pampeanas (Bense et al., 2013).

Along with the Cuchilla Dionisio Terrane and Punta del Este Terrane, another important source of zircons for the Chaco-Paraná Basin samples (LMF-3, LMF-2, LMF-5, LP-3, AND-1) appears to be recycled Devonian sediments on the Rio de la Plata Craton whose provenance was described by Uriz et al. (2016). This is particularly true of sample AND-1, which is from an outcrop of the San Gregorio Formation located just west of Devonian Durazno Group outcrops (Fig. 2B). The age distribution of zircons in sample AND-1 is quite different from the other Chaco-Paraná Basin samples that were analyzed, with a higher percentage of Mesoproterozoic grains (34% compared to 7%, 4%, 0%, and 8%) (Fig. 8) but is very similar to sample UC-13 (Uriz et al., 2016) of the Durazno Group, which was collected ~80 km to the east from AND-1. Both the K–S test and cross-correlation coefficient ($R^2 = 0.60$) support the likelihood that the Durazno Group was the primary source of sediments in AND-1 (Table 2). This indicates a different drainage network, flowing towards the west, for Location 4. Interestingly, AND-1 also has similar provenance to NOM (Nomtsas Formation, Nama Group) from the Nama Basin in Namibia and NAM-325 (Dwyka Group) from the Aranos Basin in Namibia (Table 2, Figs. 9 and 10) (Blanco et al., 2011; Zieger et al., 2019). In particular, the KDE's of AND-1 and NAM-325 show similar peaks and peak intensities (Fig. 7). The likely explanation for these similarities is that Permian Dwyka Group, the Devonian Durazno Group, and the Cambrian Nomtsas Formation have similar provenance with all three samples consisting of zircons derived from the Cuchilla Dionisio Terrane and Namaqua Terrane in Africa (part of the Cargonian Highlands). However, this interpretation cannot be verified without additional supporting data. It also seems plausible that the Nama Basin sediments were eroded and resedimented into the eastern Chaco-Paraná Basin during the LPIA and were possibly mixed with resedimented Devonian sediments. The similar detrital zircon signatures of the San Gregorio Formation in Uruguay (AND-1) and the Dwyka Group in southern Namibia (NAM-325, Zieger et al., 2019) suggests a possible link between glaciation in these locations. However, there are also some key differences between the Dwyka Group and San Gregorio Formation ages, including the lack of Archean ages in sample AND-1 compared to the Dwyka Group sample. Also, sample AND-1 appears to have a slightly younger Cambrian peak. Although many of the ages presented in the San Gregorio Formation samples can be attributed to purely Uruguayan sources, the fact that these sources can be limited to terranes east and southeast of the study locations strongly implies that ice advanced west and northwest out of the known African highlands.

An alternative source for the Chaco-Paraná Basin sediments in Uruguay that has to be ruled out is the RGS in southern Brazil. Although grooved surfaces and glaciotectonized sediments on the RGS indicate ice flow towards the north and northwest, some authors have hypothesized a small ice-cap on the RGS that drained south into the Chaco-Paraná Basin (e.g. Santos et al., 1996; Rocha-Campos et al., 2008). When looking at the RGS, the primary Neoproterozoic peak detected from sample SUS-1 (Itararé Group) is ~680 Ma with a secondary peak at ~780 Ma. These peaks and their relative heights are similar to sample STR (Itararé Group) from Griffis et al. (2019a) and sample GG (Guaritas Group) from Oliveira et al. (2014), which are also from the RGS (Fig. 5). The relatively high cross-correlation coefficients support a similar provenance for SUS-1, STR, and GG (Table 2). Thus, it seems most likely that the Precambrian/Cambrian Camaquã Basin sediments (Guaritas Group) were easily eroded by northward flowing glaciers and resedimented across the RGS during the late Paleozoic. Other possible sources for SUS-1 in southern Brazil or northern Uruguay include the Neoproterozoic São Gabriel Terrane (~600–900 Ma) or the Archean to Paleoproterozoic Taquarembó and Rivera Terranes (~2–2.55 Ga) (e.g. Gastal et al., 2005; Saalmann et al., 2005; Hartmann et al., 2011). Griffis et al. (2019a) also concluded that STR was mostly derived from the Guaritas Group due to the fact that the Itararé Group directly overlies these strata and their detrital zircon ages are very similar. Meanwhile, Itararé Group sediments described in other studies of paleovalleys on the eastern RGS exhibit a detrital zircon age signature with a single ~600 Ma peak that matches the underlying Pelotas Batholith (Fedorchuk et al., 2019b; Tedesco et al., 2019).

The K–S test indicates different provenance for the RGS samples and the Chaco-Paraná Basin samples (Table 1). Only LMF-5 (the post-glacial Tres Islas Formation) has a relatively high cross-correlation coefficient when compared to the RGS (Table 2). Furthermore, the RGS samples (SUS-1, GG, and STR) lack the slightly younger ~520–555 Ma peak common in the Chaco-Paraná Basin samples (LMF-3, LMF-2, LMF-5, LP-3, AND-1) (Figs. 5 and 6). The RGS samples also contain more Paleoproterozoic grains compared to the Chaco-Paraná Basin samples (Fig. 8). Based on this data, we hypothesize that the RGS was not a major source of sediment to the Chaco-Paraná Basin samples analyzed here. However, it should be noted that the MDS indicates similarity between SUS-1 and samples LMF-3 and LMF-2 (the San Gregorio Formation) from Uruguay (Fig. 10). This may indicate that some sediment from Uruguay was transported north onto the RGS during glaciation and mixed with the Camaquã Basin sediments, although this connection seems tenuous.

6.2. Late Paleozoic sediment dispersal patterns

This study shows trends in the detrital zircon age distributions that correspond to shifts in drainage and/or the position of subglacial erosion between ice-proximal, relatively ice-distal, and post-glacial sediments. For example, in the sample LMF-3 (Location 2) of diamictite from the San Gregorio Formation that directly overlies glacially carved basement features (i.e. ice-proximal sediments), there is a higher proportion of ages that reflect the underlying syn-tectonic granites (Figs. 6 and 11). This supports local erosion and deposition at the study locations during the glacial maximum. In the KDE, this is represented by a dominance of the older ~625 Ma peak over the younger ~520–555 Ma peak (post-tectonic granites) (Figs. 6 and 11) (Blanco, 2009; Basei et al., 2011). Meanwhile, LMF-2 was collected in the slightly more ice-distal (glaciomarine) sandstones of the San Gregorio Formation at the same sample location. These sandstones contain iceberg keel marks and are stratigraphically ~15 m above sample LMF-3 (Fig. 4). In contrast, to sample LMF-3, LMF-2 contains a dominant younger ~520–555 Ma peak which is probably derived from zircons of the post-tectonic granite intrusions to the east and southeast of the study area (Figs. 6 and 11). The orientation of subglacially carved whaleback structures supports this interpretation by suggesting that ice advanced from the southeast towards the northwest (Fig. 4). This indicates that when ice retreated to the east and southeast the location of subglacial erosion shifted to the new ice margin and a wider fluvial drainage catchment opened up. As a result, more young zircons were transported to and deposited at Location 2 (Fig. 11). This interpretation is also supported by sample LP-3 which is from the glaciomarine Cerro Pelado Formation at Location 3. Similar to LMF-2, LP-3 also shows a dominant younger ~520–555 Ma peak over the older ~625 Ma peak, which supports a wider drainage for this glaciomarine sample (Figs. 6 and 11). The similar provenance of samples LMF-2 and LP-3 is supported by the K–S test (Table 1), the MDS

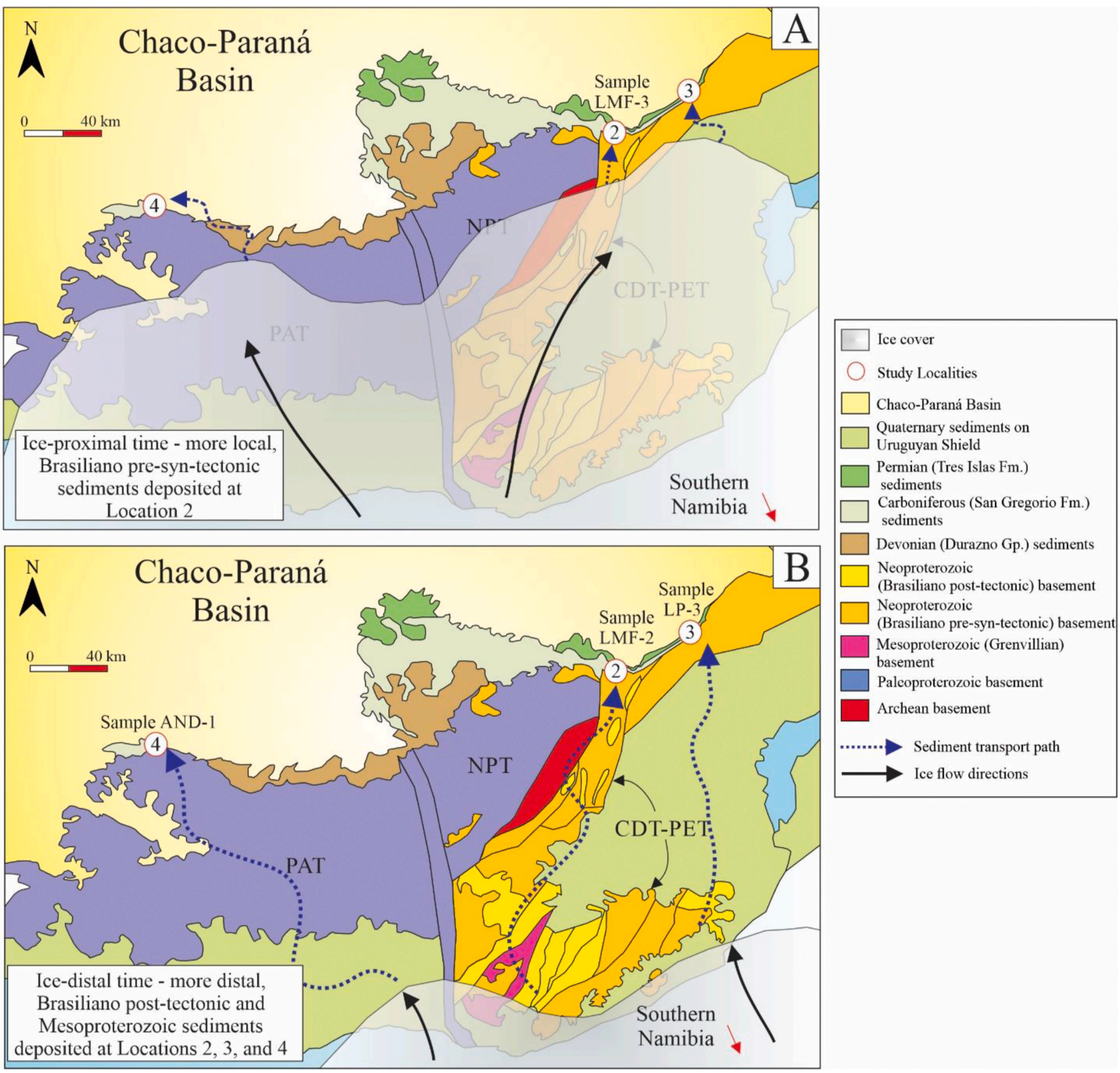

Fig. 11. Interpretation of sediment dispersal during ice-proximal and distal glacial times after Loureiro et al. (2017) and Blanco et al. (2009). (A) Dispersal during ice-proximal times. Detrital zircons primarily reflect local Brasiliano pre- and syn-tectonic sediments at Location 2 (sample LMF-3). (B) Interpretation of sediment dispersal pattern during ice-distal time. Detrital zircons (samples AND-1, LMF-2, LP-3) reflect larger drainage catchment that includes more Brasiliano post-tectonic sources and Mesoproterozoic sources, possibly in Africa. Note different sediment pathway for Location 4 compared to Locations 2 and 3.

(Fig. 10), and the cross-correlation coefficient ($R^2 = 0.76$) (Table 2), which indicate that these samples are most similar to each other. A similar trend was observed for ice-proximal/ice-distal sediments in the eastern Paraná Basin by Griffis et al. (2019a). The study by Griffis et al. (2019a) also noted the shift to more diverse and exotic zircons from Africa in ice-distal glaciomarine facies and less diverse and more local South American zircons in ice-proximal facies. It should be noted that AND-1 has a unique detrital zircon signature compared to the other Chaco-Paraná Basin samples, and likely represents a different drainage pathway (Fig. 11).

At Location 2, the postglacial (fluvial-deltaic) Tres Islas Formation is comprised of arkosic, cross-bedded, fluvial sandstones. Paleocurents within the Tres Islas Formation described here demonstrate flow towards the southwest and southeast (Fig. 4), which suggests a different provenance for these sediments compared to those deposited during ice-proximal or ice-distal glacial times. Sample LMF-5 was collected from one of these sandstones (Fig. 4). The detrital zircon age distribution shows a similarity to the ice-proximal sample LMF-3 with a dominant ~625 Ma peak and lack of diverse grains (Fig. 6). The K–S P-value and cross-correlation coefficient ($R^2 = 0.58$) both support a close relationship between LMF-5 and LMF-3 (Table 2). This similarity reflects a return to primarily local provenance (Fig. 2B). The abundance of locally sourced sediment may be the result of fluvial incision driven by a drop in base level, tectonically driven uplift, or glacial rebound (isostatic uplift) during postglacial times.

6.3. Ice center and paleogeographic reconstructions

The detrital zircon ages measured from the eastern Chaco-Paraná Basin at Locations 2, 3, and 4 all reflect sources in eastern and southeastern Uruguay (Fig. 2B), and possibly southwestern Namibia (Fig. 1A). This indicates that most of the sediments were likely transported towards the west and northwest, out of present Africa or southeast Uruguay during the late Paleozoic. Grooved surfaces and whalebacks at Location 2 also indicate thick, fast-flowing ice moved towards the northwest (Figs. 4 and 12A) (e.g. Assine et al., 2018). This is further supported by previous studies of glacial deposits and grooved surfaces in Africa that show an ice center over the Cargonian Highlands of southern Namibia and South Africa that drained into adjacent basins, including a westward flow towards the Chaco-Paraná Basin (Fig. 12B) (e.g. Visser, 1989; 1997b; Dietrich and Hofmann, 2019; Le Heron et al., 2019; Zieger et al., 2019). The detrital zircon ages detailed here represent a similar drainage pattern to that responsible for deposition of the Devonian Durazno Group as reported by Uriz et al. (2016), who also hypothesized a catchment that included the highlands of southeastern Uruguay and southern Namibia. This implies that this area was a persistent source area since the Devonian.

Meanwhile, grooved surfaces and glaciotectonic deformation on the RGS (southernmost Brazil) show a pattern of ice flow to the north, northeast, and northwest (Fig. 12A) (e.g. Tomazelli and Soliani Júnior 1982, 1997; Fedorchuk et al., 2019a). This aligns with the hypothesis that the southern Namibian based ice center extended north and northwest across southeast Uruguay and onto the RGS as an unconfined lobe (Fig. 12B). However, the detrital zircon ages from the San Gregorio Formation in the eastern Chaco-Paraná Basin are quite different from the Itararé Group on the RGS. Some authors have proposed a small isolated ice center on the RGS that drained radially outward (e.g. Santos et al., 1996; Rocha-Campos et al., 2008). However, based on this study and the abundance of paleo-ice flow indicators showing flow to the north and northwest, the most likely explanation for the different provenance is that the abundance of easily-erodible Precambrian/Cambrian Camaquã Basin sediments contributed most of zircons to the Itararé Group on the RGS and diluted any Uruguayan signature. Additionally, the zone of maximum subglacial erosion may have shifted north of Uruguayan basement sources during glaciation of the RGS. Meanwhile, previous detrital zircon studies have suggested that the Itararé Group on the eastern margin of the Paraná Basin (north of the RGS, in Paraná and Santa Catarina States) have a northern Namibian provenance (e.g. Canile et al., 2016; Griffis et al., 2019a). Samples from the eastern Paraná Basin have dominant Mesoproterozoic peaks that are quite different than those from both the RGS (e.g. Griffis et al., 2019a) and the eastern Chaco-Paraná Basin. This supports the interpretation that sediments deposited on the eastern margin of the Paraná Basin have a different provenance from those on the southernmost margin of the Paraná Basin (RGS) and the Chaco-Paraná Basin (e.g. Fedorchuk et al., 2019b; Griffis et al., 2019a; Tedesco et al., 2019).

This study provides the first U–Pb detrital zircon geochronologic constraints on LPIA rocks from the Chaco-Paraná Basin of Uruguay. Findings support the hypothesis that unconfined ice extended out of southeastern Uruguay (and likely southwestern Namibia) into the eastern Chaco-Paraná Basin and southernmost Paraná Basin (Fig. 12B). The U–Pb detrital zircon signature of the LPIA sediments in this region is distinct from that observed along the eastern Paraná Basin, which is sourced from northern Namibia, suggesting a separate catchment (e.g. Frakes and Crowell, 1972; Crowell and Frakes, 1975; Griffis et al., 2019a). This contradicts both the hypothesis of a single massive ice center that uniformly glaciated the Paraná and Chaco-Paraná Basins and the hypothesis of a small, isolated ice cap on the RGS (e.g. Santos et al., 1996; Gesicki et al., 1998; Gesicki et al., 2002; Rocha-Campos et al., 2008). This provides some evidence that glaciers preferentially persisted in separate African highlands during warm intervals, and emanated out of these areas when the paleoclimate cooled (e.g. Isbell et al., 2012). Furthermore, while the detrital zircon ages described in this study primarily reflected local sources, clear differences in sediment dispersion were noted between ice-proximal, relatively ice-distal glaciomarine, and post-glacial sediments. This may be related to the shifting position of subglacial erosion or drainage changes related to isostatic adjustments such as the formation of an isostatic trough during glacial advance and rebound of this trough as ice retreated. This may also have occurred in conjunction with the blockage and opening of preglacial drainage systems as ice advanced and retreated over the study area. These environment-specific differences in detrital zircon signatures may have important implications for interpreting how detrital zircons are distributed on glacially-influenced margins. Therefore, future detrital zircon studies of late Paleozoic glacial deposits should account for the possibility of regional and environmental variability when making interpretations of sediment provenance.

7. Conclusions

1. The San Gregorio and Cerro Pelado Formations, as well as the Tres Islas Formation, from the eastern Chaco-Paraná Basin in Uruguay have a different provenance than the glacial sediments (Itararé Group) on the RGS in southernmost Brazil.
2. The detrital zircon samples collected from late Paleozoic strata in the Chaco-Paraná Basin primarily reflect source terranes in east and southeast Uruguay or Africa such as the Cuchilla Dionisio Terrane, Punta del Este Terrane, and the Namaqua Belt. The Devonian Durazno Group is also a likely source for these sediments.
3. The detrital zircon sample (SUS-1) of the Itararé Group collected from the RGS has a similar provenance to another Itararé Group sample collected from elsewhere on the RGS reported by Griffis et al. (2019a). This sample also has a similar provenance to the Precambrian/Cambrian Guaritas Group sample (Oliviera et al., 2014) from the Camaquã Basin on the RGS. Therefore, it is hypothesized that glaciers easily eroded the Camaquã Basin strata on the RGS and redeposited those sediments across the RGS during the Carboniferous.
4. Based on the provenance of the late Paleozoic sediments from the eastern Chaco-Paraná Basin and southernmost Paraná Basin, combined with paleo-ice flow directions from other studies, the most likely scenario is that an ice center was located over southern

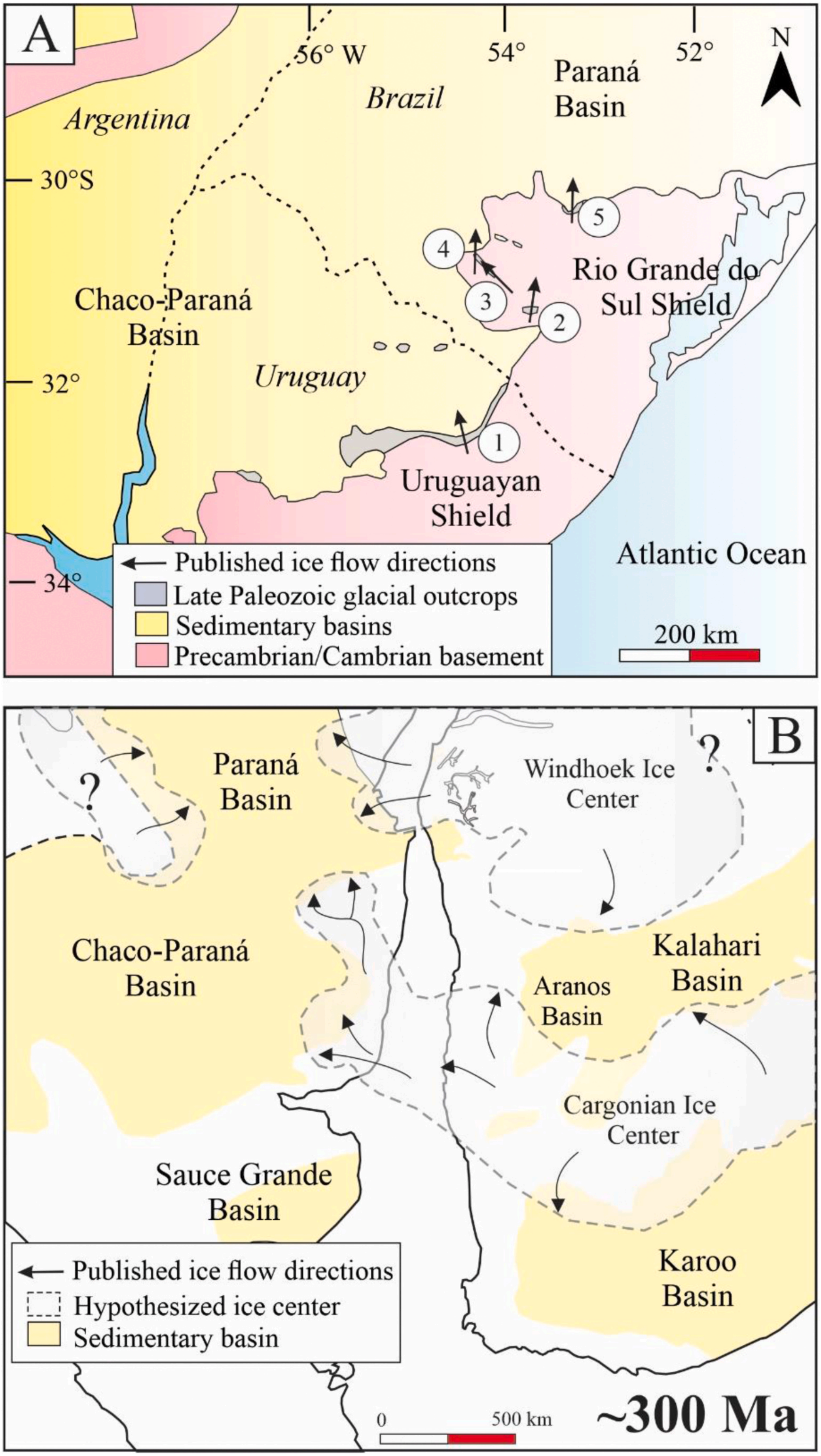

Fig. 12. Paleogeographic reconstruction of ice center that affected study area in southernmost Paraná Basin and eastern Chaco-Paraná Basin. (A) Map of study area showing published ice flow directions. (1) Assine et al. (2018). (2) Tomazelli and Soliani Júnior (1982). (3) Fedorchuk et al. (2019a). (4) Tomazelli and Soliani Júnior (1997). (5) Tomazelli and Soliani Júnior (1982). (B) Reconstruction of two hypothesized ice centers over African highlands draining into Paraná and Chaco-Paraná Basins during the Carboniferous. After Visser (1997b), Rocha-Campos et al. (2008), Uriz et al. (2016), and Assine et al. (2018).

Namibia and northern South Africa. An unconfined lobe likely flowed northwest onto the RGS and west into the Chaco-Paraná Basin from Africa. The detrital zircon ages do not support an isolated ice center over the RGS or an eastward flowing ice-center from the Sierra Pampeanas.

5. Comparison of the detrital zircon age distribution from ice-proximal, relatively ice-distal glaciomarine, and post-glacial strata indicates that changes in sediment dispersal occurred during ice advance/retreat. Ice-proximal and post-glacial fluvial strata primarily have zircons sources from local igneous basement (~625 Ma), while the relatively ice-distal glaciomarine strata contain younger zircons (~520–555 Ma) from a larger catchment to the east and southeast of the study area.
6. This study supports the interpretation that at least two catchments, sourcing different highlands in Africa, supplied sediments to the Paraná and Chaco-Paraná Basins in Brazil and Uruguay. It is hypothesized that for some period during the Carboniferous-Permian, an ice center was located over the Windhoek Highlands in northern Namibia and another was located in the Cargonian Highlands of southern Namibia and northern South Africa.

Author statement

Nicholas D. Fedorchuk: Conceptualization, methodology, investigation, formal analysis, visualization, writing – original draft, writing – review and editing. **Neil P. Griffis:** Methodology, investigation, formal analysis, writing – review and editing. **John L. Isbell:** Supervision, project administration, resources, funding acquisition, investigation, writing – review and editing. **César Goso:** Investigation, project administration, writing – review and editing. **Eduardo L.M. Rosa:** investigation, writing – review and editing. **Isabel P. Montañez:** Supervision, project administration, resources, funding acquisition, investigation, writing – review and editing. **Qing-Zhu Yin:** Resources, project administration, funding acquisition, writing – review and editing. **Magdalena H. Huyskens:** Methodology, investigation, writing – review and editing. **Matthew E. Sanborn:** Methodology, investigation. **Roland Mundil:** Supervision, funding acquisition, investigation, writing – review and editing. **Fernando F. Vesely:** Supervision, project administration, funding acquisition, investigation, writing – review and editing. **Roberto Iannuzzi:** Supervision, project administration, funding acquisition, writing – review and editing.

Declaration of competing interest

The authors declare that they have no known competing financial interests or personal relationships that could have appeared to influence the work reported in this paper.

Acknowledgements

This project was supported financially by grants from the U.S. National Science Foundation (OISE-1444181, OISE-1559231, and EAR-1729219 to JI; OISE-1444210 and EAR-1729882 to IPM), the UW-Milwaukee Research Growth Initiative (RGI), and Conselho Nacional de Desenvolvimento Científico e Tecnológico (CNPq, grants 461650/2014-2, 430096/2016-0, PQ 312747/2017-9). Other financial support was provided by the American Association of Petroleum Geologists (AAPG), the Geological Society of America (GSA), the Society for Sedimentary Geology (SEPM), the UWM Center for Latin American and Caribbean Studies (CLACS), the UWM Milwaukee Geosciences Department, the Wisconsin Geological Society, the Instituto de Ciencias Geológicas (IGC) of Faculty of Sciences (UdelaR, Uruguay), and Coordenação de Aperfeiçoamento de Pessoal de Nível Superior (CAPES).

Appendix A. Supplementary data

Supplementary data to this article can be found online at https://doi.org/10.1016/j.jsames.2020.102989.

References

Assine, M.L., de Santa Ana, H., Veroslavsky, G., Vesely, F.F., 2018. Exhumed subglacial landscape in Uruguay; erosional landforms, depositional environments, and paleo-ice flow in the context of the late Paleozoic Gondwanan glaciation. Sediment. Geol. 369, 1–12.

Basei, M.A.S., Peel, E., Sanchez Bettucci, L., Preciozzi, F., Nutman, A.P., 2011. The basement of the Punta del Este Terrane (Uruguay); an African Mesoproterozoic fragment at the eastern border of the South American Rio de La Plata Craton. Int. J. Earth Sci. 100, 289–304.

Beltan, L., 1981. Coccocephalichthys tessellatus n. sp. (Pisces, Actinopterygii) from the upper carboniferous of Uruguay. In: 2nd Congresso Latino-Americano de Paleontologia, Porto Alegre, pp. 95–105.

Bense, F.A., Löbens, S., Dunkl, I., Wemmer, K., Siegesmund, S., 2013. Is the exhumation of the Sierras Pampeanas only related to Neogene flat-slab subduction? Implications from a multi-thermochronological approach. J. S. Am. Earth Sci. 48, 123–144.

Beri, Á., Gutiérrez, P., Balarino, L., 2011. Palynostratigraphy of the late Palaeozoic of Uruguay, Paraná Basin. Rev. Palaeobot. Palynol. 167, 16–29.

Beri, Á., Gutiérrez, P.R., Balarino, M.L., 2015. The late Paleozoic palynological diversity in southernmost Paraná (Uruguay), claromecó and Paganzo basins (Argentina), western Gondwana. J. S. Am. Earth Sci. 64, 183–189.

Berry, R.F., Jenner, G.A., Meffre, S., Tubrett, M.N., 2001. a north American provenance for neoproterozoic to cambrian sandstones in Tasmania? Earth Planet Sci. Lett. 192, 207–222.

Blanco, G., Germs, G.J.B., Rajesh, H.M., Chemale Jr., F., Dussin, I.A., Justino, D., 2011. Provenance and paleogeography of the Nama Group (Ediacaran to early Palaeozoic, Namibia); petrography, geochemistry and U/Pb detrital zircon geochronology. Precambrian Res. 187, 15–32.

Blanco, G., Rajesh, H.M., Gaucher, C., Germs, G.J.B., Chemale Jr., F., 2009. Provenance of the Arroyo del Soldado Group (Ediacaran to Cambrian, Uruguay); implications for the paleogeographic evolution of southwestern Gondwana. Precambrian Res. 171, 57–73.

Bossi, J., 1966. Geología del Uruguay. Colección Ciencias. n° 2. Universidad de la República, Montevideo, p. 419.

Bossi, J., Gaucher, C., 2004. The Cuchilla Dionisio terrane, Uruguay; an allochthonous block accreted in the cambrian to SW-Gondwana. Gondwana Res. 7, 661–674.

Braun, A., Sprechmann, P., Gaucher, C., 2003. Stratigraphic age of phosphorite-nodules from the san Gregorio Formation of Uruguay. Neues Jahrbuch Geol. Palaontol. Monatsh. 12, 739–748.

Cagliari, J., Philipp, R.P., Buso, V.V., Netto, R.G., Klaus Hillebrand, P., da Cunha Lopes, R., Stipp Basei, M.A., Faccini, U.F., 2016. Age constraints of the glaciation in the Paraná Basin: evidence from new U–Pb dates. J. Geol. Soc. 173, 871–874.

Canile, F.M., Babinski, M., Rocha-Campos, A.C., 2016. Evolution of the Carboniferous-Early Cretaceous units of Parana Basin from provenance studies based on U-Pb, Hf and O isotopes from detrital zircons. Gondwana Res. 40, 142–169.

Closs, D., 1967a. Orthocone cephalopods from the upper carboniferous of Argentina and Uruguay. Ameghiniana 5, 123–129.

Closs, D., 1967b. Upper carboniferous anaptychi from Uruguay. Ameghiniana 5, 145–148.

Closs, D., 1969. Intercalation of Goniatites in the Gondwanic Glacial Beds of Uruguay. Gondwana Stratigraphy, IUGS 1st Gondwana Symposium. UNESCO, Paris, Buenos Aires, pp. 197–212.

Craddock, J.P., Ojakangas, R.W., Malone, D.H., Konstantinou, A., Mory, A., Bauer, W., Thomas, R.J., Affinati, S.C., Pauls, K., Zimmerman, U., Botha, G., Rochas-Campos, A., Tohver, E., Riccomini, C., Martin, J., Redfern, J., Horstwood, M., Gehrels, G., 2019. Detrital zircon provenance of Permo-Carboniferous glacial diamictites across Gondwana. Earth Sci. Rev. 192, 285–316.

Crowell, J., Frakes, L., 1975. The late Paleozoic glaciation. Gondwana Geology 3, 313–331.

Crowell, J.C., 1999. Pre-Mesozoic Ice Ages: Their Bearing on Understanding the Climate System, vol. 192. Geological Society of America Memoir, pp. 1–106.

DeGraaff-Surpless, K., Mahoney, J.B., Wooden, J.L., McWilliams, M.O., 2003. Lithofacies control in detrital zircon provenance studies: insights from the Cretaceous Methow Basin, southern Canadian Cordillera. Geol. Soc. Am. Bull. 115, 899–915.

De Santa Ana, H., 2004. Análise Tectono-Estratigráfica das Seqüências Permotriassica e Jurocretácea da Bacia Chacoparanense Uruguaia ("Cuenca Norte"). UNESP. PhD Dissertation, Brasil, p. 274.

De Santa Ana, H., Goso, C., Daners, G., 2006a. Cuenca Norte: estratigrafía del Carbonífero-Pérmico. In: Veroslavsky, G., Ubilla, M., Martinez, S. (Eds.), Cuencas Sedimentarias de Uruguay. Geología, Paleontología y Recursos Minerales. Facultad de Ciencias, Montevideo, pp. 147–208.

De Santa Ana, H., Veroslavsky, G., Fulfaro, V.J., Rossello, E.A., 2006b. Cuenca Norte: evolución tectónica y sedimentaria del Carbonífero-Pérmico. In: Veroslavsky, G., Ubilla, M., Martinez, S. (Eds.), Cuencas Sedimentarias de Uruguay. Geología, Paleontología y Recursos Minerales. Facultad de Ciencias, Montevideo, pp. 209–256.

Dietrich, P., Hofmann, A., 2019. Ice-margin fluctuation sequences and grounding zone wedges: the record of the late Paleozoic ice age in the eastern Karoo basin (Dwyka Group, South Africa). The Depositional Record 5, 247–271.

Du Toit, A.A., 1927. A Geological Comparison of South America with South Africa, vol. 381. Carnegie Institute of Washington, p. 157.
Du Toit, A.A., 1937. Our Wandering Continents, an Hypothesis of Continental Drifting. Oliver and Boyd, Edinburgh, p. 355.
Fallgatter, C., Paim, P.S.G., 2017. On the origin of the Itararé Group basal nonconformity and its implications for the late Paleozoic glaciation in the Paraná Basin, Brazil. Palaeogeogr. Palaeoclimatol. Palaeoecol. 531 (Part B).
Fedorchuk, N.D., Isbell, J.L., Griffis, N.P., Vesely, F.F., Rosa, E.L.M., Montãnez, I.P., Mundil, R., Yin, Q.-Z., Iannuzzi, R., Roesler, G., Pauls, K.N., 2019a. Carboniferous glaciotectonized sediments in the southernmost Paraná Basin, Brazil. Ice marginal dynamics and paleoclimate indicators. Sediment. Geol. 389, 54–72.
Fedorchuk, N.D., Isbell, J.L., Griffis, N.P., Montañez, I.P., Vesely, F.F., Iannuzzi, R., Mundil, R., Yin, Q.-Z., Pauls, K.N., Rosa, E.L.M., 2019b. Origin of paleovalleys on the Rio Grande do Sul Shield (Brazil): implications for the extent of late Paleozoic glaciation in west-central Gondwana. Palaeogeogr. Palaeoclimatol. Palaeoecol. 531 (Part B).
Fielding, C.R., Frank, T.D., Isbell, J.L., 2008. The late Paleozoic ice age–A review of current understanding and synthesis of global climate patterns. In: Fielding, C.R., Frank, T.D., Isbell, J.L. (Eds.), Resolving the Late Paleozoic Ice Age in Time and Space, vol. 441. Geological Society of America Special Paper, pp. 343–354.
Fielding, C.R., Frank, T.D., Isbell, J.L., Henry, L.C., Domack, E.W., 2010. Stratigraphic signature of the late Palaeozoic ice age in the Parmeener Supergroup of Tasmania, SE Australia, and inter-regional comparisons. Palaeogeogr. Palaeoclimatol. Palaeoecol. 298, 70–90.
Frakes, L., Crowell, J., 1972. Late Paleozoic glacial geography between the Paraná Basin and the Andean geosyncline. An Acad. Bras Ciências 44, 139–145.
Franca, A.B., Potter, P.E., 1991. Stratigraphy and reservoir potential of glacial deposits of the Itarare Group (Carboniferous-Permian), Parana basin, Brazil. AAPG (Am. Assoc. Pet. Geol.) Bull. 75, 62–85.
Frank, T.D., Shultis, A.I., Fielding, C.R., 2015. Acme and demise of the late Palaeozoic ice age: a view from the southeastern margin of Gondwana. Palaeogeogr. Palaeoclimatol. Palaeoecol. 418, 176–192.
Gastal, M.d.C.P., Lafon, J.M., Hartmann, L.A., Koester, E., 2005. Sm/Nd isotopic compositions as a proxy for magmatic processes during the Neoproterozoic of the southern Brazilian Shield. J. S. Am. Earth Sci. 18, 255–276.
Gastaldo, R.A., DiMichele, W.A., Pfefferkorn, H.W., 1996. Out of the icehouse into the greenhouse; a late Paleozoic analog for modern global vegetational change. GSA Today (Geol. Soc. Am.) 6, 1–7.
Gaucher, C., Finney, S.C., Poire, D.G., Valencia, V.A., Grove, M., Blanco, G., Pamoukaghlian, K., Gomez Peral, L., 2008. Detrital zircon ages of Neoproterozoic sedimentary successions in Uruguay and Argentina; insights into the geological evolution of the Rio de la Plata Craton. Precambrian Res. 167, 150–170.
Gesicki, A.L.D., Riccomini, C., Boggiani, P.C., 2002. Ice flow direction during late Paleozoic glaciation in western Paraná Basin, Brazil. J. S. Am. Earth Sci. 14, 933–939.
Gesicki, A.L.D., Riccomini, C., Boggiani, P.C., Coimbra, A.M., 1998. The Aquidauana formation (Parana basin) in the context of late Palaeozoic glaciation in western Gondwana. J. Afr. Earth Sci. 27, 81–82.
Goso, C., 1995. Análise estratigráfica da Formação San Gregorio na borda leste da Bacia Norte Uruguaia. UNESP. M.Sc. thesis, Brazil, p. 214.
Griffis, N.P., Mundil, R., Montañez, I.P., Isbell, J., Fedorchuk, N., Vesely, F., Iannuzzi, R., Yin, Q.-Z., 2018. A new stratigraphic framework built on U-Pb single-zircon TIMS ages and implications for the timing of the penultimate icehouse (Paraná Basin, Brazil). Geol. Soc. Am. Bull. 130, 848–858.
Griffis, N.P., Montañez, I.P., Fedorchuk, N., Isbell, J., Mundil, R., Vesely, F., Weinshultz, L., Iannuzzi, R., Gulbranson, E., Taboada, A., Pagani, A., Sanborn, M.E., Huyskens, M., Wimpenny, J., Linol, B., Yin, Q.-Z., 2019a. Isotopes to ice: constraining provenance of glacial deposits and ice centers in west-central Gondwana. Palaeogeogr. Palaeoclimatol. Palaeoecol. 531 (Part B).
Griffis, N.P., Montañez, I.P., Mundil, R., Richey, J., Isbell, J., Fedorchuk, N., Linol, B., Iannuzzi, R., Vesely, F., Mottin, T., Rosa, E., Keller, B., Yin, Q.-Z., 2019b. Coupled stratigraphic and U-Pb zircon age constraints on the late Paleozoic icehouse-to-greenhouse turnover in south-central Gondwana. Geology 47, 1146–1150.
Guillemain, C., 1911. Zur Geologie Uruguays. Z. Dtsch. Geol. Ges. 63, 203–220.
Hambrey, M.J., Glasser, N.F., 2003. Glacial sediments: processes, environments and facies. In: Middleton, G.V. (Ed.), Encyclopedia of Sediments and Sedimentary Rocks. Kluwer, Dordrecht, pp. 316–331.
Hartmann, L.A., Philipp, R.P., Santos, J.O.S., McNaughton, N.J., 2011. Time frame of 753–680 Ma juvenile accretion during the São Gabriel orogeny, southern Brazilian Shield. Gondwana Res. 19, 84–99.
Holz, M., 2003. Sequence stratigraphy of a lagoonal estuarine system; an example from the lower Permian Rio Bonito Formation, Parana basin, Brazil. Sediment. Geol. 162, 305–331.
Holz, M., Franca, A.B., Souza, P.A., Iannuzzi, R., Rohn, R., 2010. A stratigraphic chart of the Late Carboniferous/Permian succession of the eastern border of the Parana Basin, Brazil, South America. J. S. Am. Earth Sci. 29, 381–399.
Holz, M., Küchle, J., Philipp, R.P., Bischoff, A.P., Arima, N., 2006. Hierarchy of tectonic control on stratigraphic signatures: base-level changes during the Early Permian in the Paraná Basin, southernmost Brazil. J. S. Am. Earth Sci. 22, 185–204.
Holz, M., Souza, P.A., Iannuzzi, R., 2008. Sequence stratigraphy and biostratigraphy of the late carboniferous to early Permian glacial succession (Itarare Subgroup) at the eastern-southeastern margin of the Parana basin, Brazil. Spec. Pap. Geol. Soc. Am. 441, 115–129.
Isbell, J.L., Miller, M.F., Wolfe, K.L., Lenaker, P.A., 2003. Timing of late Paleozoic glaciation in Gondwana: was glaciation responsible for the development of northern hemisphere cyclothems?. In: Chan, M.A., Archer, A.W. (Eds.), Extreme Depositional Environments: Mega End Members in Geologic Time, vol. 370. Geological Society of America Special Paper, pp. 5–24.
Isbell, J.L., Henry, L.C., Gulbranson, E.L., Limarino, C.O., Fraiser, M.L., Koch, Z.J., Ciccioli, P.L., Dineen, A.A., 2012. Glacial paradoxes during the late Paleozoic ice age: evaluating the equilibrium line altitude as a control on glaciation. Gondwana Res. 22, 1–19.
Lawver, L.A., Dalziel, I.W.D., Norton, I.O., Gahagan, L.M., 2011. The Plates 2011 Atlas of plate reconstructions (500 Ma to present day). Plates Progress Report No. 345-0811. University of Texas, p. 189. Technical Report No. 198.
Le Heron, D.P., Dietrich, P., Busfield, M.E., Kettler, C., Bermanschläger, S., Grasemann, B., 2019. Scratching the surface: footprint of a late Carboniferous ice sheet. Geology 47, 1034–1038.
Limarino, C.O., Spalletti, L.A., 2006. Paleogeography of the upper Paleozoic basins of southern South America: an overview. J. S. Am. Earth Sci. 22, 134–155.
Limarino, C.O., Césari, S.N., Spalletti, L.A., Taboada, A.C., Isbell, J.L., Geuna, S., Gulbranson, E.L., 2014. A paleoclimatic review of southern South America during the late Paleozoic: a record from icehouse to extreme greenhouse conditions. Gondwana Res. 25, 1396–1421.
Lopez Gamundi, O.R., 1997. Glacial-postglacial Transition in the Late Paleozoic Basins of Southern South America. Oxford University Press, New York, NY.
Loureiro, J., Bettucci, L.S., Cerdán, F.P., Spoturno, J., 2017. Mapa Geológico del Uruguaya escala 1:500.000. http://visualizadorgeominerodinamige.gub.uy/DINAMIGE_mvc2/.
Mallmann, G., Chemale Jr., F., Avila, J.N., Kawashita, K., Armstrong, R.A., 2007. Isotope geochemistry and geochronology of the Nico Perez terrane, Rio de la Plata Craton, Uruguay. Gondwana Res. 12, 489–508.
Marques-Toigo, M., 1970. Anabaculites nov. gen., a new miospore genus from San Gregorio Formation of Uruguay. Ameghiniana 7, 79–82.
Marques-Toigo, M., 1974. Some new species of spores and pollens of lower Permian age from the san Gregorio Formation in Uruguay. An. Acad. Bras. Cienc. 46, 601–616.
Martin, H., 1981. The late Palaeozoic Dwyka Group of the south Kalahari Basin in Namibia and Botswana and the subglacial valleys of the Kaokoveld in Namibia. In: Hambrey, M.J., Harland, W.B. (Eds.), Earth's Pre-pleistocene Glacial Record. Cambridge University Press, Cambridge, UK, pp. 61–66.
Martin, J.R., Redfern, J., Horstwood, M.S.A., Mory, A.J., Williams, B.P.J., 2019. Detrital zircon age and provenance constraints on late Paleozoic ice-sheet growth and dynamics in Western and Central Australia. Aust. J. Earth Sci. 66, 183–207.
Montañez, I.P., Soreghan, G., 2006. Earth's fickle climate: lessons learned from deep-time ice ages. Geotimes 51, 24.
Montañez, I.P., Poulsen, C.J., 2013. The late Paleozoic ice age: an evolving paradigm. Annu. Rev. Earth Planet Sci. 41, 629–656.
Mottin, T.E., Vesely, F.F., Rodrigues, M.C.N.L., Kipper, F., Souza, P.A., 2018. The paths and timing of late Paleozoic ice revisited: new stratigraphic and paleo-ice flow interpretations from a glacial succession in the upper Itararé Group (Paraná Basin, Brazil). Palaeogeogr. Palaeoclimatol. Palaeoecol. 490, 488–504.
Oliveira, C.H.E., Chemale, F., Jelinek, A.R., Bicca, M.M., Philipp, R.P., 2014. U–Pb and Lu–Hf isotopes applied to the evolution of the late to post-orogenic transtensional basins of the dom feliciano belt, Brazil. Precambrian Res. 246, 240–255.
Raymond, A.L., Metz, C., Parrish, J.T., 2004. Ice and its consequences; glaciation in the late ordovician, late devonian, Pennsylvanian-Permian, and cenozoic compared. J. Geol. 112, 655–670.
Rocha-Campos, A.C., dos Santos, P.R., Canuto, J.R., 2008. Late Paleozoic glacial deposits of Brazil; Parana basin, 441. Special Paper - Geological Society of America, pp. 97–114.
Rosa, E.L.M., Vesely, F.F., Isbell, J.L., Kipper, F., Fedorchuk, N.D., Souza, P.A., 2019. Constraining the timing, kinematics and cyclicity of mississippian-early Pennsylvanian glaciations in the Paraná Basin, Brazil. Sediment. Geol. 384, 29–49.
Rosa, E.L.M., Vesely, F.F., França, A.B., 2016. A review on late Paleozoic ice-related erosional landforms in the Paraná Basin: origin and paleogeographical implications. Braz. J. Genet. 46, 147–166.
Saalmann, K., Gerdes, A., Lahaye, Y., Hartmann, L.A., Remus, M.V.D., aLaeufer, A., 2011. Multiple accretion at the eastern margin of the Rio de la Plata Craton; the prolonged Brasiliano Orogeny in southernmost Brazil. Int. J. Earth Sci. 100, 355–378.
Saalmann, K., Remus, M.V.D., Hartmann, L.A., 2005. Geochemistry and crustal evolution of volcano-sedimentary successions and orthogneisses in the Sao Gabriel Block, southernmost Brazil; relics of Neoproterozoic magmatic arcs. Gondwana Res. 8, 143–161.
Saalmann, K., Remus, M.V.D., Hartmann, L.A., 2006. Tectonic evolution of the Neoproterozoic Sao Gabriel Block, southern Brazil; constraints on Brasiliano orogenic evolution of the Rio de la Plata cratonic margin. J. S. Am. Earth Sci. 21, 204–227.
Santos, P.R., Rocha-Campos, A.C., Canuto, J.R., 1996. Patterns of late Palaeozoic deglaciation in the Paraná Basin, Brazil. Palaeogeogr. Palaeoclimatol. Palaeoecol. 125, 165–184.
Saylor, J.E., Knowles, J.N., Horton, B.K., Nie, J., Mora, A., 2013. Mixing of source populations recorded in detrital zircon U-Pb age spectra of modern river sands. J. Geol. 121, 17–33.
Saylor, J.E., Stockli, D.F., Horton, B.K., Nie, J., Mora, A., 2012. Discriminating rapid exhumation from syndepositional volcanism using detrital zircon double dating; implications for the tectonic history of the Eastern Cordillera, Colombia. Geol. Soc. Am. Bull. 124, 762–779.
Saylor, J.E., Sundell, K.E., 2016. Quantifying comparison of large detrital geochronology data sets. Geosphere 12, 203–220.
Schneider Santos, J.O., Hartmann, L.A., Bossi, J., Campal, N., Schipilov, A., Pineyro, D., McNaughton, N.J., 2003. Duration of the trans-Amazonian cycle and its correlation

within south America based on U-Pb SHRIMP geochronology of the La Plata Craton, Uruguay. Int. Geol. Rev. 45, 27–48.

Starck, D., Papa, C.d., 2006. The northwestern Argentina Tarija Basin: stratigraphy, depositional systems, and controlling factors in a glaciated basin. J. S. Am. Earth Sci. 22, 169–184.

Tedesco, J., Cagliari, J., Coitinho, J.d.R., da Cunha Lopes, R., Lavina, E.L.C., 2016. Late Paleozoic paleofjord in the southernmost Parana Basin (Brazil); geomorphology and sedimentary fill. Geomorphology 269, 203–214.

Tedesco, J., Cagliari, J., Chemale Júnior, F., Girelli, T.J., Lana, C., 2019. Provenance and paleogeography of the southern Paraná Basin: geochemistry and U—Pb zircon geochronology of the Carboniferous-Permian transition. Sediment. Geol. 393–394, 105539.

Tomazelli, L.J., Soliani Júnior, E., 1982. Evidências de atividade glacial no Paleozóico Superior do Rio Grande do Sul, Brasil. Anais II Congresso Brasileiro de Geologia, Salvador 4, 1378–1389.

Tomazelli, L.J., Soliani Júnior, E., 1997. Sedimentary facies and depositional environments related to Gondwana glaciation in batovi and Suspiro regions, Rio Grande do Sul, Brazil. J. S. Am. Earth Sci. 10, 295–303.

Uriz, N.J., Cingolani, C.A., Basei, M.A.S., Blanco, G., Abre, P., Portillo, N.S., Siccardi, A., 2016. Provenance and paleogeography of the devonian Durazno Group, southern Parana Basin in Uruguay. J. S. Am. Earth Sci. 66, 248–267.

Vermeesch, P., Resentini, A., Garzanti, E., 2016. An R package for statistical provenance analysis. Sediment. Geol. 336, 14–25.

Vesely, F.F., Assine, M.L., 2006. Deglaciation sequences in the permo-carboniferous Itarare Group, Parana basin, southern Brazil. J. S. Am. Earth Sci. 22, 156–168.

Vesely, F.F., Trzaskos, B., Kipper, F., Assine, M.L., Souza, P.A., 2015. Sedimentary record of a fluctuating ice margin from the Pennsylvanian of western Gondwana; Parana Basin, southern Brazil. Sediment. Geol. 326, 45–63.

Visser, J.N.J., 1989. The permo-carboniferous Dwyka formation of southern Africa: deposition by a predominantly subpolar marine ice sheet. Palaeogeogr. Palaeoclimatol. Palaeoecol. 70, 377–391.

Visser, J.N.J., 1997a. Deglaciation sequences in the Permo-Carboniferous Karoo and Kalahari basins of Southern Africa; a tool in the analysis of cyclic glaciomarine basin fills. Sedimentology 44, 507–521.

Visser, J.N.J., 1997b. A review of the Permo-Carboniferous glaciation in Africa. In: Martini, I.P. (Ed.), Late Glacial and Postglacial Environmental Changes: Quaternary, Carboniferous-Permian, and Proterozoic. Oxford University Press, Oxford, UK, pp. 169–191.

Winn Jr., R.D., Steinmetz, J.C., 1998. Upper Paleozoic strata of the Chaco-Paraná basin, Argentina, and the great Gondwana glaciation. J. S. Am. Earth Sci. 11, 153–168.

Zieger, J., Stutzriemer, M., Hofmann, M., Gärtner, A., Gerdes, A., Marko, L., Linnemann, U., 2020. The evolution of the southern Namibian Karoo-aged basins: implications from detrital zircon geochronologic and geochemistry data. Int. Geol. Rev. https://doi.org/10.1080/00206814.2020.1795732.

Zieger, J., Rothe, J., Hofmann, M., Gärtner Linnemann, U., 2019. The Permo-Carboniferous Dwyka Group of the Aranos Basin (Namibia) – how detrital zircons help understanding sedimentary recycling during a major glaciation. J. Afr. Earth Sci. 158, 103555.